

Chapter 10: Organic-inorganic semiconductor heterojunctions for hybrid light-emitting diodes

Author(s):

*J. Bruckbauer (Department of Physics, SUPA, University of Strathclyde, Glasgow, Scotland, United Kingdom, jochen.bruckbauer@strath.ac.uk)

N. J. Findlay (WestCHEM, School of Chemistry, University of Glasgow, Scotland, United Kingdom, neil.findlay@glasgow.ac.uk)

10.1 Introduction

The beginning of the 21st century saw a transformation from conventional light sources to solid-state lighting (SSL) [1, 2]. Conventional light sources such as incandescent light bulbs, almost unchanged since its invention in the 1800s, and fluorescent tubes are either highly inefficient in converting electricity into light or can often contain toxic materials. In the early 1990s, crucial breakthroughs in the improvements of nitride semiconductors by three Japanese scientists enabled the realisation of highly efficient blue light-emitting diodes (LEDs) [3]. This was recognised with the 2014 Nobel Prize in Physics “*for the invention of efficient blue light-emitting diodes which has enabled bright and energy-saving white light sources*” [4].

White light emission using LEDs can be achieved by different methods [2, 5]: Combining inorganic LEDs of multiple wavelengths; combining an inorganic LED with a suitable colour converter or using purely organic electroluminescent materials. The most commonly used and commercially established approach is the combination of a blue LED and a yellow-emitting phosphor. Issues with phosphors generated a strong drive towards phosphor-free LEDs. These issues include challenging colour tuning and rendering, availability of green and red phosphors, self-absorption and use of expensive rare-earth materials [6, 7].

Organic LEDs (OLEDs) are made entirely of luminescent organic or organometallic molecules [8]. Their thin film deposition allows the fabrication of large area and flexible devices. The

absorption and emission properties of these organic materials can be directly influenced and tuned by modifying and adjusting their chemical structure [9].

In this chapter, a different approach is presented which utilises the ‘best of both worlds’ through combining the ultra-high efficiency of inorganic nitride-based LEDs with the flexibility and low-cost of organic energy-down converters. The first part (section 10.2) will cover the basic principles of inorganic LEDs and give an introduction to colorimetry, radiometry and efficiency of light sources. This is followed by a short overview on the chemical design considerations for the organic compound in section 10.3. In section 10.4 examples of light-emitting polymers will be given. Finally, the main section (10.5), illustrates the versatility of small molecules as organic colour converters.

10.2 Basic introduction to white LEDs

10.2.1 III-nitride semiconductors and inorganic LEDs

The III-nitride semiconductor material system consists of the materials gallium nitride (GaN), indium nitride (InN) and aluminium nitride (AlN) along with their alloys. This material family has gained a lot of interest due to the band gap tunability of the ternary (e.g. InGaN and AlGaN) and quaternary alloys (e.g. InAlGaN) from the deep ultraviolet (UV) to the near infrared wavelength regions [10, 11]. By alloying GaN with InN it is possible to cover the entire visible spectrum, whereas alloying GaN with AlN allows the band gap to be shifted into the UV spectral region. Figure 1(a) illustrates the spectral range covered by the III-nitrides showing the room temperature band gap of wurtzite AlN, GaN and InN plotted against their a -lattice constant [12]. The most common crystal structure for the III-nitrides is the thermodynamically stable hexagonal wurtzite structure as shown in Figure 1(b), which is defined by the a - and c -lattice constants [13].

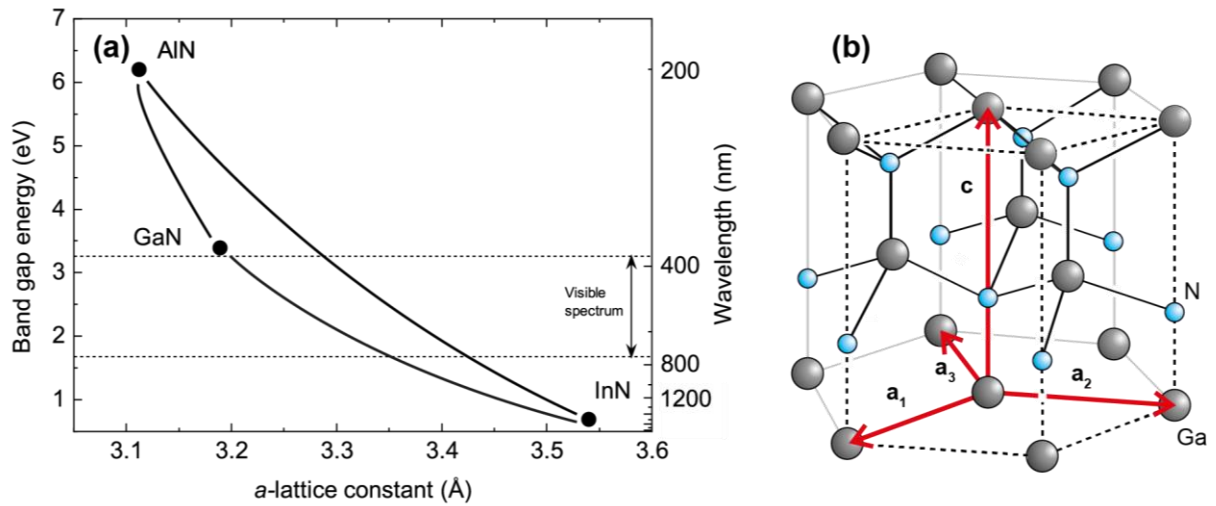


Figure 1 (a) Band gap energy versus a-lattice constant of wurtzite AlN, GaN and InN at room temperature. (b) Thermodynamically stable hexagonal wurtzite structure of GaN.

The basic building block of an LED is a p-n junction consisting of a p- and n-type doped semiconductor [14]. In an unbiased p-n junction in thermal equilibrium electrons originating from donors on the n-side diffuse towards the p-side where they recombine with holes. The same process happens with holes diffusing to the n-side. This creates a depletion region in the vicinity of the junction devoid of free carriers. Ionised donors and acceptors (the dopants), however, stay behind forming a space charge region, which creates an electric field across the junction. This electric field counteracts the diffusion current and leads to a drift current of electrons (holes) from the p-side (n-side) to the n-side (p-side). In thermal equilibrium both currents cancel each other, meaning there is no total current flowing across the junction. Figure 2(a) shows the bending of the conduction and valance bands caused by the internal electric field, which represents a barrier for free carriers. In the case of a positively biased p-n junction (forward bias) the externally applied electric field opposes the internal field and lowers the barrier created by it. Injected free carriers diffuse across the junction into the region of opposite conductivity and recombine there by emitting

light as shown in Figure 2(b). In the case of a negatively biased p-n junction the potential barrier is increased and no current flows across the junction.

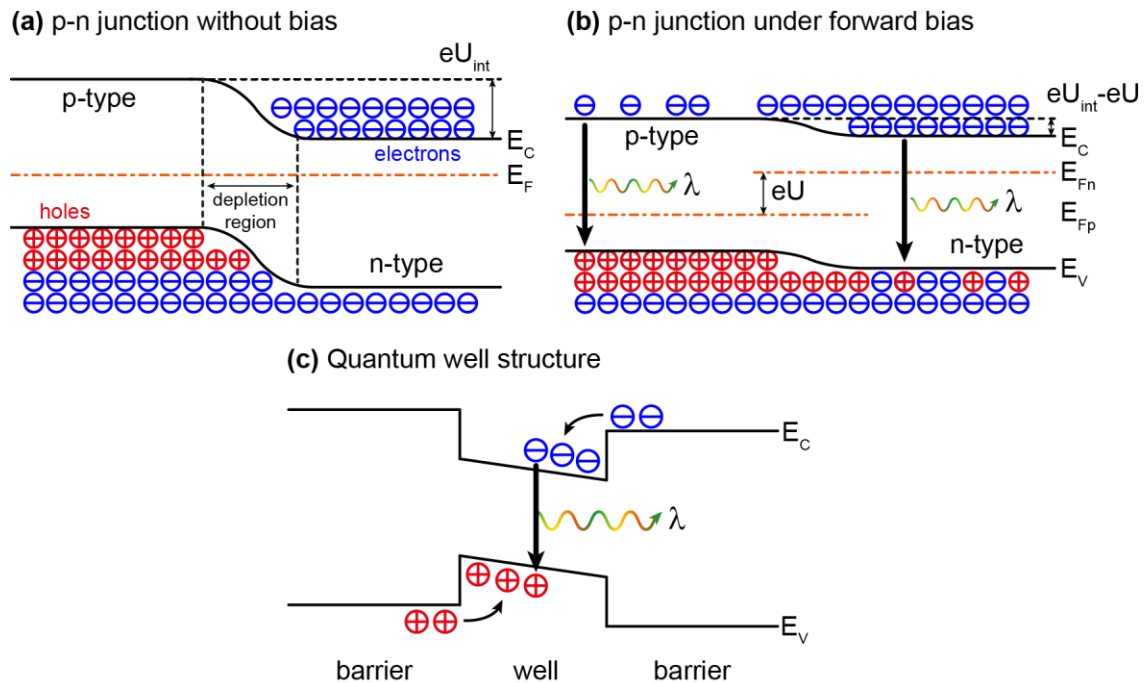


Figure 2 (a) p-n junction without bias with U_{int} caused by the internal electric field, (b) p-n junction under forward bias U and (c) quantum well structure. E_C and E_V denote the conduction and valence bands, respectively.

The area in a p-n junction where recombination occurs is defined by the diffusion length, which is the mean distance a carrier diffuses until recombination. This reduces the electron (n) and hole densities (p) and hence the radiative recombination rate. To make the recombination process more efficient most modern LEDs possess a quantum well (QW) structure (also referred to as the active region), which is a semiconductor with lower band gap (well), positioned between the p- and n-type semiconductor of larger band gaps (barrier) as displayed in Figure 2(c). In the case of a blue LED, the well layer consists of InGaN with an alloy composition giving a band gap in the blue region and GaN barrier layers. Here injected carriers are trapped or confined to the well region, because of the lower potential. The QW width is generally around a few nanometers and therefore

much smaller than the diffusion length, which is 50–60 nm in GaN and could be up to a few tens of μm in the case of GaAs [15-18]. The result is a higher carrier density, which is proportional to the radiative recombination rate $R \propto np$ (n and p are the electron and hole densities, respectively) in comparison with a p-n junction where the area is defined by the diffusion length. LEDs commonly consist of multiple wells to further increase confinement, which is referred to as a multiple quantum well (MQW) structure.

10.2.2 Colorimetry, radiometry, photometry and efficacy

The “science of colour”, or *colorimetry*, describes the quantification and perception of light by the human eye. Unlike other physical quantities, the perception of light is a subjective quantity, depending strongly on each individual. To standardise the measurement of colours, the *Commission Internationale de l'Eclairage* (CIE, International Commission for Illumination) has introduced the chromaticity diagram [19], which essentially describes the quality of colour. It uses three colour-matching functions to calculate the chromaticity coordinates x and y , which span the chromaticity diagram. The colour-matching functions correspond to the response of the three cone cells in the human eye, which are sensitive in the red, green and blue spectral range. Additionally, the response of the human eye is taken into account by defining the green colour-matching function to be identical to the *eye sensitivity function* $V(\lambda)$ (CIE 1978), which has its maximum at 555 nm [20]. The red and blue colour-matching functions are mathematically transformed into a new set with the green colour-matching function fixed. Any spectrum can be described by these colour-matching functions, with three *tristimulus values* X , Y and Z specifying the contribution of each colour-matching function. The chromaticity coordinates x , y and z are calculated by normalising the tristimulus values according to:

$$x = \frac{X}{X + Y + Z} \quad (10.1)$$

$$y = \frac{Y}{X + Y + Z} \quad (10.2)$$

$$z = \frac{Z}{X + Y + Z} = 1 - x - y \quad (10.3)$$

The z chromaticity coordinate is redundant, because it can be calculated from the x and y chromaticity coordinates and does not provide any additional information, therefore colour is defined by a simple (x, y) coordinate system.

It was shown that the CIE 1931 chromaticity diagram (x, y) , Figure 3(a), possesses small elliptical areas of colour, which appear identical to the human eye [21]. Taking these geometrical features into account, the modified CIE 1976 (u', v') uniform chromaticity diagram was introduced, which is shown in Figure 3(b) [22]. Monochromatic light (as indicated) can be found on the perimeter, whereas white light is located in a region close to the centre of the diagram. Every colour can be described by chromaticity coordinates, i.e. its location in the chromaticity diagram. Although the light from inorganic LEDs is almost monochromatic, it has a spectral linewidth. The coordinates of LEDs, therefore, can be found in close proximity to the perimeter of the chromaticity diagram. If the linewidth becomes broader the location moves towards the centre of the diagram, such as for white light, which covers most of the visible spectrum.

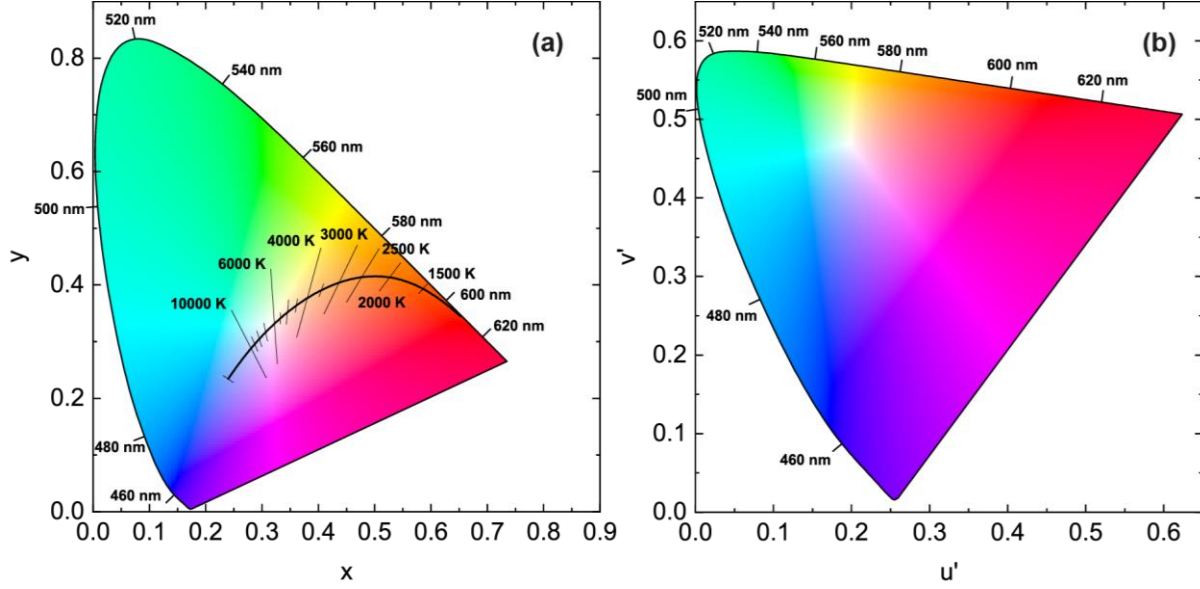


Figure 3 (a) CIE 1931 (x, y) chromaticity diagram and (b) CIE 1976 (u', v') uniform chromaticity diagram. Monochromatic colour is located on the perimeter, whereas white light is close to the centre of the diagram. The Planckian locus for colour temperatures between 1500 K and 10000 K is also shown.

White light can be generated from a combination of numerous potential spectra. To characterise white light, defined standards are used. One unique standard is the *Planckian black body radiator*, because it can be described with only one parameter, namely the colour temperature T . The black body spectrum $I(\lambda)$ is described by *Planck's law* [23, 24]:

$$I(\lambda) = \frac{2hc^2}{\lambda^5 \left(e^{\frac{hc}{\lambda k_B T}} - 1 \right)} \quad (10.4)$$

where h is the Planck constant, c the speed of light, k_b the Boltzmann constant and T the temperature and λ the wavelength of the body. Figure 4 shows Planckian black body spectra for various temperatures. The maximum of the peak can be described by *Wien's displacement law* [25]

$$\lambda_{\max} = \frac{2889 \mu\text{m K}}{T} \quad (10.5)$$

With increasing temperature, the maximum of the peak shifts towards shorter wavelengths. The

temperature T , also referred to as *colour temperature* can be used to describe the emission spectra of a Planckian black body radiator.

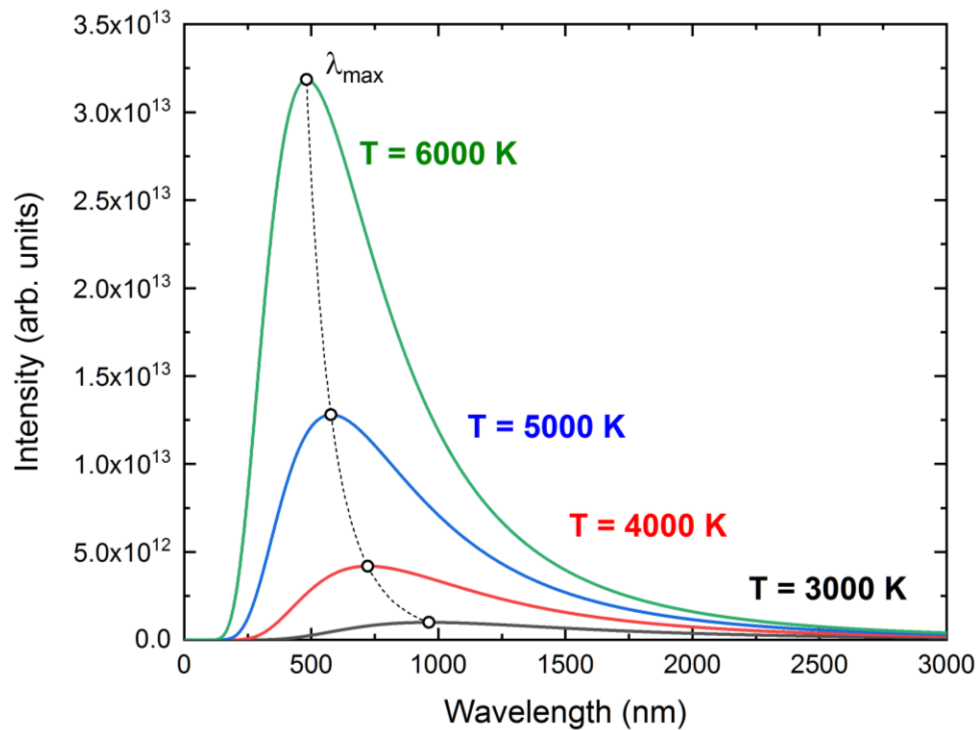


Figure 4 Intensity distribution of a Planckian black body radiator as a function of wavelength λ for different colour temperatures T . The position of the maximum (λ_{\max}) is described by Wien's law.

Each Planckian black body spectrum for different colour temperatures can be described with chromaticity coordinates, spanning a curve in the chromaticity diagram. This curve is known as the *Planckian locus*, displayed in Figure 3(a). The spectrum of a black body with very low colour temperatures contains more infrared light and its location in the chromaticity diagram can be found near the perimeter of red light. With increasing colour temperature, the spectrum shifts into the range of the visible light and the position in the chromaticity diagram moves to the region where white light is located.

The term colour temperature stems from the fact that, with increasing temperature, a black body

glows red, orange, yellow, white, and then blueish. Therefore, the *colour temperature* (unit: K) of a white light source corresponds to the temperature of a Planckian black body radiator of the same chromaticity coordinates. Not all white light sources, however, can be described with a Planckian black body radiator, i.e. they are not located exactly on the Planckian locus. Hence, the *correlated colour temperature* (CCT, unit: K) of a white light source is the temperature of a black body radiator whose colour has the best resemblance to the white light source [26]. The choice of white light with a certain CCT depends strongly on individual preference. In Japan white light with higher CCTs (around 5000 K) describing cold white light is preferred, whereas warm white light (CCTs below 3000 K) is generally desired in the UK and US [27].

A true white light source needs to have the ability to reproduce the real colour of the illuminated object accurately. The *colour rendering index* (CRI) is a measure of the ability of a light source to render or reproduce the colour of an object faithfully in comparison with the light of an ideal or natural source [22, 28]. The CRI is dimensionless, and its maximum value is 100, representing an ideal colour rendering source. The CRI is an important parameter to describe the quality of a light source. Light sources in homes or offices should have high colour rendering capabilities (high CRI), whereas colour rendering is less crucial (lower CRI) for street lights or lights for general illumination. The CRI of a Planckian black body radiator is defined to have the highest colour rendering capabilities (CRI of 100), because it most closely resembles natural daylight. The closest light source to a black body radiator is the incandescent light bulb, which (as a black body emitter) has the highest possible CRI of 100, as a consequence all other light sources have a lower CRI.

Radiometry describes the science of the measurement of electromagnetic radiation, which includes visible light. For LED characterisation, the radiant flux $\Phi_{\text{rad}}(\lambda)$ is an important quantity. It describes the total radiant energy per unit time and is measured in Watts (W).

Photometry on the other hand is the measurement of light taking the human eye response into account. Similar to the radiant flux, the luminous flux Φ_{lum} , measured in lumen (lm), describes the total power perceived by the human eye; essentially, how bright a light source appears. It can be calculated from the radiant flux by taking the eye sensitivity function $V(\lambda)$ into account using the following equation:

$$\Phi_{\text{lum}}(\lambda) = 683 \frac{\text{lm}}{\text{W}} \int_{\lambda} V(\lambda) \Phi_{\text{rad}}(\lambda) d\lambda \quad (10.6)$$

For the characterisation of white light generation, the *luminous efficacy* is an important parameter, which defines the efficiency of the energy conversion. The luminous efficacy is defined as the ratio of the luminous flux and power, with units in lumen per Watt (lm/W). For the *luminous efficacy of optical radiation*, the power is equivalent to the radiant flux of the device. More commonly, the *luminous efficacy of a light source* is used, where the power corresponds to the electrical input power of the light source.

The luminous efficacy is a general parameter describing the efficacies of white light sources. Recently, another parameter was introduced for characterising white LEDs using blue LEDs [29]. The *blue-to-white (B-W) efficacy* is the ratio of the luminous flux of the white LED to the radiant flux of the underpinning blue LED. This efficacy essentially describes how much of the optical power of the blue LED is converted into perceived white light, i.e. luminous flux, by the specific colour converter. Commercial phosphor-based converters have values above 200 lm/W.

10.2.3 White light generation

The light emitted by LEDs is defined by the band gap of the semiconductor. Commonly, there are two approaches used to achieve white light. Either a combination of inorganic LEDs emitting at different wavelengths is used or a single blue or UV LED is coated by a down-converting material.

White light can be generated by different combinations of emission spectra as described below.

The trivial approach is using two or more LEDs on separate chips, each emitting nearly monochromatic light, which when combined emit white light. When using two LEDs (*dichromatic*) their wavelengths have to be complementary and operate at a certain power ratio in order to be perceived as white. Dichromatic white LEDs in general have high luminous efficacy (ratio of luminous flux to power in units of lumen per watt), but a low colour rendering index. The CRI can be improved by adding more LEDs of different emission wavelengths (e.g. *trichromatic*) however its luminous efficiency will decrease [2, 5]. This is a fundamental trade-off between the colour rendering capabilities and the luminous efficiency of an LED, which cannot be eliminated. Examples would be a blue and yellow LED or a combination of three LEDs emitting in the red, green and blue (RGB) spectral regions.

Currently, the most common approach for inorganic white LEDs, consists of a single LED, emitting in the UV or the visible spectrum, coated with one or more energy down-converting phosphors. The most commonly used combination is a blue LED, using InGaN/GaN MQWs as the active region, pumping a yellow-emitting phosphor, such as YAG:Ce, to provide the requisite white light.

The conversion efficiency using a converter is limited by two factors. Firstly, the external quantum efficiency (EQE) η_{EQE} of the phosphor describes the ratio of the numbers of photons emitted and absorbed by the converter. The EQE is also the product of the internal quantum efficiency (IQE) η_{IQE} and extraction efficiency $\eta_{extraction}$:

$$\eta_{EQE} = \eta_{IQE} \cdot \eta_{extraction} \quad (10.7)$$

The IQE is the intrinsic efficiency of the converter material. The second limitation is the Stokes shift, which is an inherent energy loss due to the conversion of the absorbed photon with

wavelength λ_1 to the emitted photon with wavelength λ_2 ($\lambda_1 < \lambda_2$). This energy loss is fundamental, cannot be overcome and is given by:

$$\Delta E = E_1 - E_2 = hc \left(\frac{1}{\lambda_1} - \frac{1}{\lambda_2} \right) \quad (10.8)$$

The efficiency of the wavelength conversion can be expressed as:

$$\eta_{\text{Stokes}} = \frac{E_2}{E_1} = \frac{\lambda_1}{\lambda_2} \quad (10.9)$$

The total efficiency of the conversion process of the wavelength converter is the product of the EQE and efficiency of the wavelength conversion:

$$\eta_{\text{converter}} = \eta_{\text{EQE}} \cdot \eta_{\text{Stokes}} = \eta_{\text{EQE}} \cdot \frac{\lambda_1}{\lambda_2} \quad (10.10)$$

Due to the additional energy loss from the Stokes shift, white LEDs employing a phosphor for the conversion process show lower efficiencies than white LEDs using multiple single LEDs of different colours. The highest energy losses occur when UV light is converted into red light. Materials suited as wavelength converters include phosphors, organic dyes and semiconductors. The EQE for each of these converters can be close to 100%.

An extensive introduction on the principle of LEDs, and their operation, design, packaging and applications can be found in Refs. [2, 5].

10.2.4 Use of phosphors in white LEDs

Phosphors possess a broad emission band making them very suitable for white light generation and are very stable. They are made of an inorganic host doped with an optically active element. Common hosts are garnets, such as yttrium aluminium garnet (YAG), $\text{Y}_3\text{Al}_5\text{O}_{12}$ [30, 31]. The optically active element can be a rare earth element, rare earth oxide or other rare earth compound. For white light generation cerium (Ce) is used, whereas neodymium (Ny) is utilised for lasers. By

adding gadolinium (Gd) and/or gallium (Ga) to fabricate Ce-doped $(Y_{1-x}Gd_x)_3(Al_{1-y}Ga_y)_5O_{15}$ the emission of the phosphor can be shifted [32]. This makes it possible to change and adapt the chromaticity of the white light when used together with a blue LED. For the fabrication of white LEDs, the YAG phosphor is incorporated in epoxy resin. The epoxy is then deposited on the blue LED die. The fraction of the absorbed blue light by the phosphor depends on the thickness of the epoxy-phosphor layer and its concentration, which also defines the yellow emission intensity of the phosphor.

Issues of phosphors include challenging colour tuning and rendering, self-absorption due to overlap of broad absorption and emission bands, lack of suitable red phosphors and use of expensive rare-earth materials [6, 7].

10.2.5 White organic LEDs

White light can also be produced using entirely organic electroluminescent materials. Advantages of white organic LEDs (WOLEDs/OLEDs) include low-cost fabrication, ease of processability, fabrication of large area flexible sheets and tuning of their emission properties through modification of the chemical structure [8, 33, 34]. In order to generate white light, emissive materials of varying colour need to be combined, which can be achieved by several approaches [9]. One approach uses several individual emitters arranged in a multilayer structure, or by blending individual emitters into a single layer or by doping a host material with emissive materials at varying concentrations [35-37]. Alternatively, a single molecule can be used to generate white light by emission from its excited state and its aggregates (e.g. excimers or exciplexes) [38]. Similarly, electroluminescent polymers can be used as the emissive material [34]; however, their efficiencies are below that of multilayer WOLEDs.

10.3 Chemistry

Perhaps the most attractive feature of organic materials is the wide variety of structures obtainable, and made possible through incorporation of different, readily accessible building blocks. This allows key properties to be controlled and manipulated to achieve the desired performance, including solubility, energy gap and optoelectronic properties. There are significant seminal contributions on how to do this, and comprehensive overviews can be found in Refs. [39-41]. Here a brief discussion of key parameters as support for the remainder of this chapter will be given.

One feature common to all organic down-converting materials is that each generally contains a conjugated skeletal backbone, consisting of an alternating pattern of single and double bonds between carbon and/or heteroatoms. Often this takes the form of cyclic (and heterocyclic) rings connected either through C–C bonds, bridging double bonds or fusion of two rings together. The variety of structures available when designing organic materials for any application, including here as down-conversion units, is vast and ensures that fine control of structure and therefore application properties is possible on selection of the most appropriate candidate. Examples of selected synthetic building blocks are shown in Figure 5.

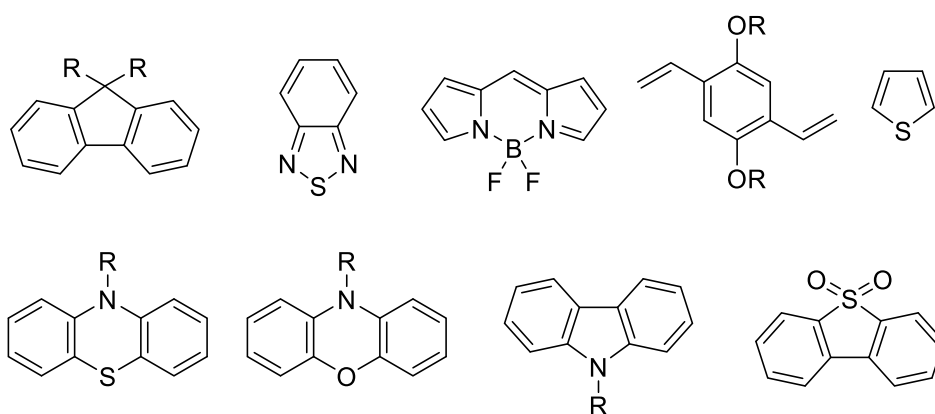


Figure 5 Examples of selected organic building blocks.

Often the most important parameter to control is the absorption and emission wavelengths to enable appropriate absorption of emitted LED light, as well as emission of the desired wavelength to achieve the sought-after hybrid light output [42-44]. Strategies to achieve this include incorporating structural units responsible for absorption and emission within a larger molecule or polymer, or introducing electron-rich and electron-poor components adjacent to each other to control the band gap, and hence the optoelectronic properties. Hybrid white light emitting LEDs rely on yellow emissive organic materials in conjunction with an efficient blue inorganic LED for example. Therefore, combining yellow emissive organic materials with blue light absorbing materials in one structure, linked via an appropriate conjugated bridge, can produce the desired output.

A further key factor that needs to be considered is the solubility of the organic species, which can require consideration of the deposition method. For example, the deposition of organic emissive active layers within OLED devices typically involves either solution processing, for example spin-coating or drop-casting, or vacuum deposition [45]. However, this either requires that a specific solvent is used to deposit the material, which can damage the existing LED structure (or underlying electronics), or the molecule can survive high temperatures and vacuum to be deposited via sublimation. An alternative method is encapsulation in a non-emissive matrix and offers several advantages. A low concentration of the bulk solution for deposition (i.e., 0.5–1% w/v) can be used, while matrices are often cured swiftly through UV light irradiation. Finally, often the existing solution-state optical properties are maintained, with minimal effects from aggregation or other morphological changes, ensuring a uniform and smooth down-conversion layer to boost the overall efficiency of the device [46].

An additional consideration is whether to employ polymers or small molecules as the organic

converting layer within a hybrid device. Both types of material have their advantages. For example, organic small molecules are monodisperse allowing for absolute identification of structure and therefore synthesis is straightforward to replicate. They also benefit from being effectively tuneable in terms of their properties via synthetic manipulation of their structure, although many materials require extensive, multi-step pathways to achieve the required product in high purity. On the other hand, polymers suffer from being polydisperse and batch-to-batch reproducibility is often challenging to achieve, although their production is more synthetically straightforward than monodisperse small molecules [47].

Overall, choice of material family is dependent on the factors outlined above and requires careful consideration prior to commencing the work.

10.4 Light-emitting polymers

10.4.1 Introduction

Light-emitting or luminescent polymers are one choice of organic colour converters. They have several advantages over currently used phosphors [33, 48, 49]. Polymers with emission characteristics covering the entire visible spectrum are available. They can have low or negligible self-absorption to due large Stokes shift between their absorption and emission peaks and can exhibit high photoluminescence quantum yields (PLQYs). They are easily dissolved in solution for easy and cost-efficient processing and regular spin-coating techniques. When deposited on bendable substrates (e.g. plastics), polymers are also flexible. Issues of polymers include stability of their emission properties and lifetime. A review on polymers used for OLEDs can be found in Refs. [34, 50, 51]. For a polymer to be emissive and therefore useful in hybrid light-emitting devices they must be conjugated, and therefore consist of a series of alternating single and double

bonds. There are an unlimited number of ways to connect polymers together (see section 10.3), but the polymer structure must enable crucial factors including solubility and high PLQY. Control of the synthetic method and therefore polymer structure also allows for close control of the energy (band) gap, either through incorporation of pendant functionalities and/or a donor-acceptor backbone and can provide fine control of the absorption and emission characteristics of the hybrid device.

This section shows different examples of combining a UV or blue-emitting nitride-based LED with either a combination of polymers or with polymers combined with other colour converter components.

10.4.2 Polymers in hybrid white LEDs

One of the first applications of an organic colour converter optically-pumped by a blue inorganic nitride-based LED was reported by Hide *et al.* utilising conjugated polymers [43]. In order to achieve white light, two conjugated polymers, both with an absorption maximum in the blue, were combined. The first emitted in the green wavelength region (BuEH-PPV) while the other emitted in the red spectral region (MEH-PPV). Their absorption and photoluminescence (PL) emission spectra can be seen in Figure 6(a) together with their chemical structures. The conjugated polymers were spin-coated either separately onto transparent glass slides or as a bilayer. Figure 6(b) shows the emission spectra of these hybrid LEDs. When separate slides of the conjugated polymers were placed above the LED, wave guiding effects occurred due to different refractive indices of the glass slide and the polymers leading to sideways emission from the glass slides reducing the forwards emission intensity. Therefore, the polymers were applied as a bilayer. Varying the thickness of the of the MEH-PVV layer allowed the control of the red and green intensity ratio and

hence the colour of the hybrid LED. As the thickness of the MEH-PVV increased more red light contributed to the overall emission and the chromaticity coordinates shifted towards the right as seen in in Figure 6(c).

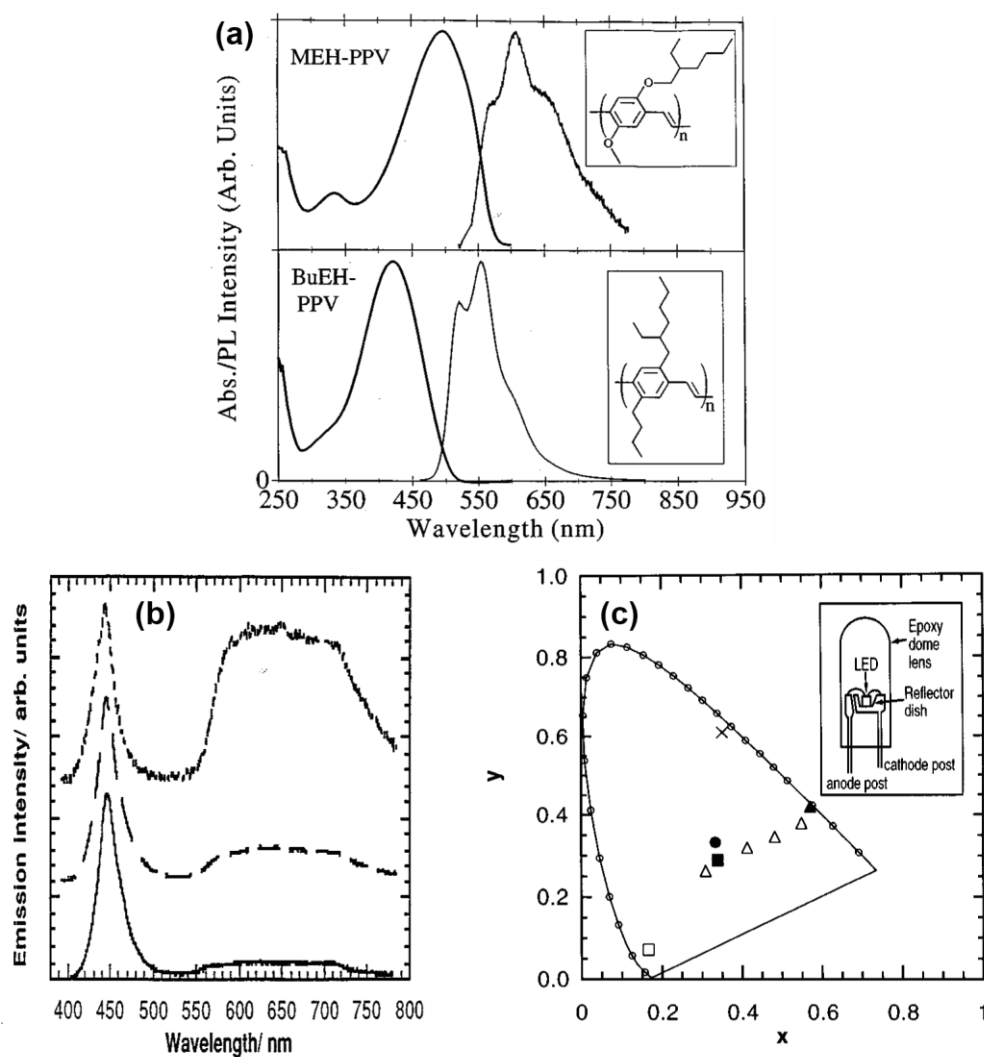


Figure 6 (a) Absorption and PL emission spectra of MEH-PVV and BuEH-PPV. Their chemical structure is shown in the insets. (b) Emission spectra of the hybrid LEDs using polymers: solid line: separate glass slides of BuEH-PPV and MEH-PVV films; dashed lines: bilayer of BuEH-PPV/MEH-PVV with two different MEH-PVV layer thicknesses. (c) CIE 1931 (x, y) chromaticity diagram: open square: blue LED; filled square and open triangles: emission from hybrid LED with BuEH-PPV/MEH-PVV bilayer with different MEH-PVV layer thicknesses; cross: PL from BuEH-PPV; solid triangle: PL from MEH-PVV. Reproduced from Ref. [43] with the permission of AIP Publishing.

One of the issues of using a colour conversion process for white light generation is the efficiency

of the energy transfer from the blue LED to the colour converter. The paper of Smith *et al.* [52] applied a commercial light-emitting polymer to a blue-emitting InGaN/GaN nanorod structure utilising non-radiative resonant energy transfer (RET). This energy transfer, also called non-radiative Förster energy transfer (FRET), relies on close coupling between the donor (the InGaN/GaN nanorod structure) to the acceptor (the light-emitting polymer) [53, 54]. The transfer rate is proportional to R^{-4} with R being the separation between a nanorod and the polymer [55]. In a regular, planar blue LED, the InGaN/GaN quantum well structure, which is the region where the blue light is emitted, is generally located over 100 nm below the surface. Therefore, the planar LED structure was etched into nanorods in order to expose the InGaN/GaN quantum wells. The polymer was then spin-coated to fill-in between the nanorods Figure 7(a) to be in direct contact with the quantum well structure for efficient FRET coupling as seen in Figure 7(b). The polymer used was the commercially available F8BT (poly[(9,9-dioctylfluorenyl-2,7-diyl)-alt-co-(1,4-benzo-{2,1',3})-thiadiazole]). PL emission spectra of only the InGaN/GaN nanorods and the hybrid structure, both measured under identical conditions using a 375 nm laser, are shown in Figure 7(c). The decay lifetimes measured at the 450 nm nanorod peak were also determined for the bare nanorod and the hybrid structure as displayed in Figure 7(d). The recombination lifetime of the hybrid structure is small due to the additional non-radiative FRET process between the nanorods and the polymer. A more detailed discussion of the lifetime measurements can be found in Ref. [52].

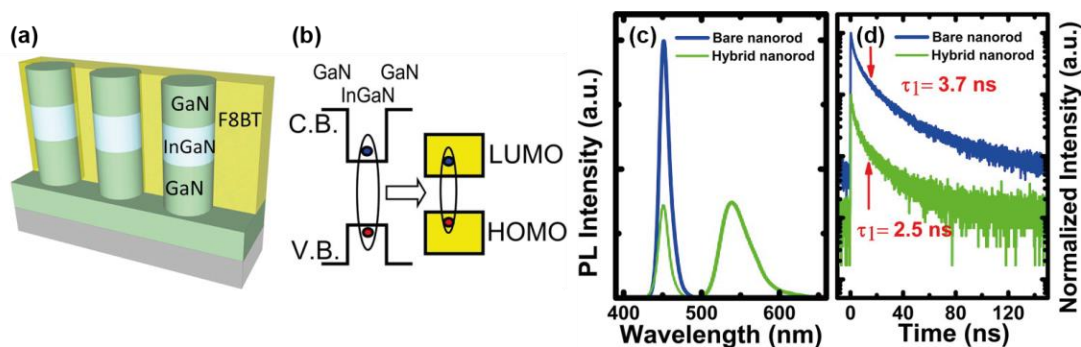


Figure 7 (a) Schematic of the hybrid structure with the polymer (F8BT) filled-in between the nanorods containing the InGaN/GaN quantum wells. (b) FRET coupling between the InGaN/GaN quantum wells and the polymer. (c) PL spectra of only the InGaN/GaN nanorods and the hybrid structure. (d) Time-resolved PL traces and decay lifetimes of the bare nanorod and hybrid structure. Adapted with permission from Ref. [52]. Copyright 2013 American Chemical Society.

Regular planer nitride LEDs typically have a dimension of $500 \mu\text{m} \times 500 \mu\text{m}$ or larger. An alternative are micro LEDs (or μ -LEDs) with dimensions in the tens of micron range [56]. The use of micro LEDs over planar LEDs has several advantages, including matrix addressable pixel for display applications and visible light communication [57, 58]. In the paper by Heliotis *et al.* light from an array of UV-emitting micro LEDs was converted using three organic polyfluorene compounds emitting at different wavelengths [59]. The UV LED consisted of an array of 60×60 micro LEDs with a diameter of $20 \mu\text{m}$ emitting at about 370 nm that could be individual addressed, while the UV-absorbing polymers consisted of the blue-emitting F8DP (poly(9,9-dioctylfluorene-co-9,9-di(4-methoxy)phenylfluorene)), the green-emitting F8BT (poly(9,9-dioctylfluorene-co-benzothiadiazole)) and the red-emitting Dow Red F copolymer. The emission from these polymer films, spin-coated on quartz substrates and placed above the micro LED array, can be seen in Figure 8(a) showing emission across the entire visible spectrum. To produce white light, the three compounds (in toluene solution) were blended at different concentrations. The emission spectra and chromaticity coordinates of four hybrid LEDs using four different mixing concentrations are shown in Figure 8(b) and (c), respectively. Hybrid LEDs A, C and D appeared white to the eye,

whereas LED B was yellowish-white. The CIE 1931 chromaticity coordinates of LED D were (0.30, 0.34), making it close to pure white which has the coordinates (0.33, 0.33). The energy transfer of these systems is assisted by non-radiative FRET. It should be noted that F8DP was the host polymer due to its lowest emission wavelength (highest energy) and energy could be transferred to the other two polymers (F8BT and Dow Red F) which possessed an absorption peak at the emission of F8DP. However, the energy transfer is more complicated than this since Dow Red F had an additional absorption peak at the emission of F8BT. Although challenging, this chain of energy transfers provides a successful route for controlling the white light emission.

The same group has demonstrated a much simpler system combining an array of blue-emitting micro LEDs (diameter of 50 μm) with a yellow-emitting conjugated copolymer (“Super Yellow”) [60], emulating the commonly used blue LED and yellow phosphor approach of commercial white LEDs. Another advantage of organic polymers over inorganic phosphors is their short luminescence lifetimes. The long lifetimes of phosphors (on the order of μs) pose a limit to achieve high data transmission rates for visible light communication [61].

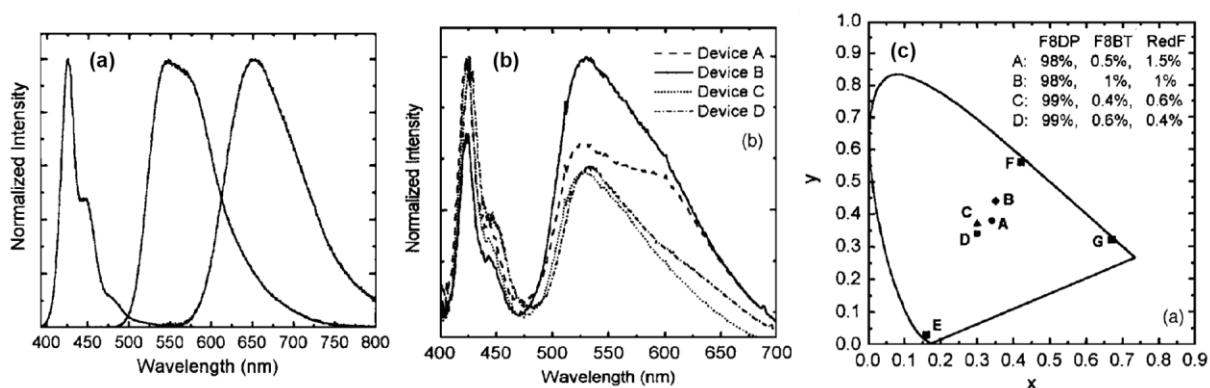


Figure 8 (a) Normalised emission spectra from F8DP, F8BT and Dow Red F (left to right) placed on top of the micro LED array. (b) Emission spectra of four hybrid LEDs (A-D) using four different blending concentrations. The concentrations in wt % are shown in (c). (c) CIE 1931 (x, y) coordinates of these four hybrid LEDs. The CIE coordinates of the LEDs only using F8DP, F8BT and Dow Red F (E, F and G) are also shown. Reproduced from Ref. [59] with the permission of AIP Publishing.

An often encountered issue of white LEDs is the lack of red emission leading to blue-ish or cool

appearing white light described by high CCTs. Although red-emitting phosphors are available they are less common compared with phosphors of other colours with lower wavelength. Chen *et al.* synthesised a novel red-emitting cationic iridium(III) coordination polymer and combined it with a standard yellow YAG:Ce phosphor in a silicone encapsulant coated on an inorganic blue LED [62]. The excitation spectra of the coordination polymer as a powder and in silicone are both quite broad, extending from the UV to the green spectral range with strong absorption in the blue spectral range as seen in Figure 9(a). The emission spectrum when excited with blue light is displayed in Figure 9(a) with an emission maximum at 620 nm and 652 nm. Hybrid LEDs were prepared by blending different concentrations (0–0.3 wt %) of the coordination polymer with YAG:Ce at a fixed concentration of 7.0 wt % in silicone. The emission spectra and chromaticity coordinates of these hybrid LEDs are shown in Figure 9(b) and (c), respectively. By adding up to 0.3 wt % of the coordination polymer the CCT could be shifted from 6157 K, with only YAG:Ce, to 3475 K with a slight change in CRI (from 72.7 to 75.6).

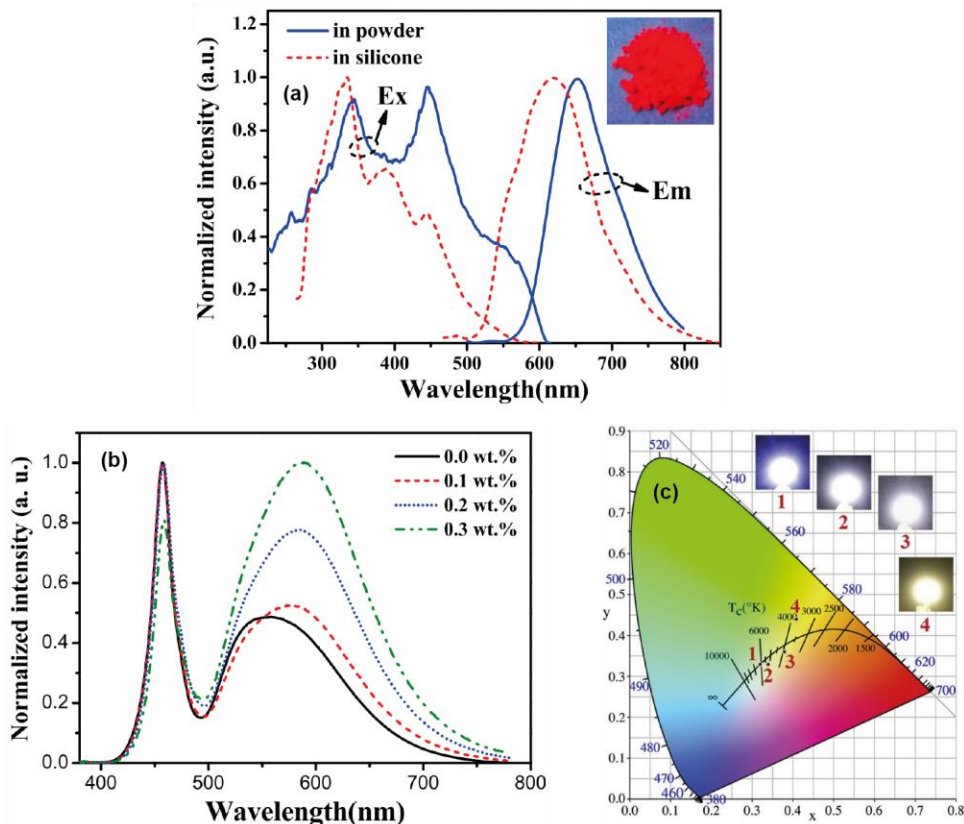


Figure 9 (a) Excitation (detection wavelength 620 nm or 653 nm) and emission (excitation wavelength 450 nm) spectra of the coordination polymer in powder form or in silicone. (b) Emission spectra and (c) chromaticity coordinates of the hybrid LEDs using different concentrations of the coordination polymer (0–0.3 wt %) and the YAG:Ce phosphor (7.0 wt %). This article was published in Ref. [62], Copyright Elsevier (2018).

The previous example combined the traditionally-used phosphor and a polymer as colour converters. Another possibility is combining an organic polymer and inorganic quantum dots (QDs). Quantum dots have the advantage of easy tunability of their emission wavelength by changing their sizes and offer high efficiencies [63]. Compared with organic materials, the emission from quantum dots is also much narrower allowing better control of the colour mixing with high colour rendering [64]. Demir *et al.* combined a UV LED with a combination of a blue-emitting polyfluorene (9,9-*bis*(2-ethylhexyl)polyfluorene) and three quantum dots (or nanocrystals as they refer to them), emitting at different wavelengths for fine-tuning of the overall white light emission [65]. The quantum dots are commercial CdSe/ZnS core-shell structures of different

diameters (2.4 nm, 3.2 nm and 5.2 nm) emitting at 540 nm, 580 nm and 620 nm, respectively. The emission spectra of the polyfluorene polymer and the quantum dots are displayed in Figure 10(a). The converter material was applied to the LED using a layer-by-layer deposition in order of increasing emission wavelength. It was shown that the CRI increased from 53.4 for the polymer and yellow-emitting quantum dot (580 nm) combination to 83.0 when all three quantum dots were used. Simultaneously, the CCT was lowered from 6762 K to 3433 K, changing the white emission from cool to warm. The emission spectrum of the hybrid LED using the polymer and all three quantum dots under different drive currents and the chromaticity coordinates are shown in Figure 10(b).

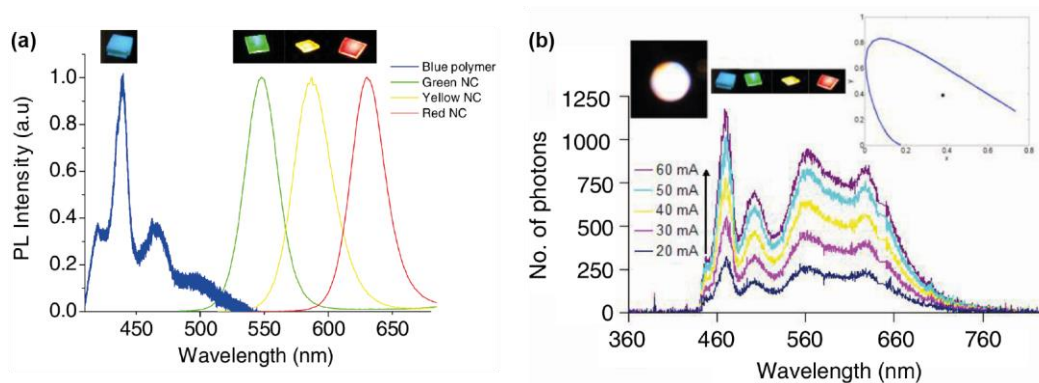


Figure 10 (a) Emission spectra of the polyfluorene polymer and the three quantum dot structures. (b) Emission spectra of the hybrid LED under different drive currents and chromaticity coordinates. Adapted and reprinted with permission under Creative Commons from Ref. [65].

10.5 Luminescent small molecules

10.5.1 Introduction

An alternative class of organic colour converter are luminescent small molecules. Much like polymers, a huge variety of structural choice is available when designing luminescent small molecules (see section 10.3 for details). This degree of choice allows for the full colour spectrum

to be achieved, while absolute control over the synthesis process ensures that the materials are monodisperse and therefore entirely reproducible. Additionally, this can lead to control of the energy gap and, through choice of appropriate sub-units, can minimise self-absorption and maximise the Stokes shift between the absorbing and emissive components. One issue that small molecule emitters can suffer from is aggregation, although often the attachment of solubilising groups can render this as ineffective to the overall device characteristics. Perhaps the main issue that small molecules can suffer from is that they can become synthetically complex, leading to questions around their long-term commercial suitability. A review on small molecules used in OLED structures can be found in Ref. [34].

This section showcases selected examples of luminescent small molecules as colour converters in hybrid LEDs, with a particular focus on how structural evolution can lead to enhanced device properties. It then will illustrate the influence of deposition method on device fabrication before applying the organic converter to blue LEDs. This section will also be used to show how to fully characterise and understand hybrid LED devices using the methodology described in section 10.2.2. This will illustrate what properties of the colour converter influence the performance of the hybrid LED, such as luminous and B-W efficacy and colour rendering (CRI).

10.5.2 Manipulation of the chemical structure and effect on optical properties

10.5.2.1 Introduction to BODIPY

The 4,4-difluoro-4-borata-3*a*-azonia-4*a*-aza-*s*-indacene unit, or BODIPY as it is commonly known, is an organic fluorescent dye and part of the difluoro-boraindacene family. Advantages of BODIPY are its thermal and photochemical stability, high fluorescence quantum yields, large absorption and emission profiles and good solubility in various organic solvents, such as acetone

and toluene [66]. Due to its properties it has found applications in biological labelling [67], luminescence [68], dye sensitised solar cells [69] and as sensors for pH and ions [70, 71]. Its tuneable emission in the yellow spectral region makes it attractive for organic light-emitting devices [66]. BODIPY has a strong, but narrow absorption peak, which is confined to around 500 nm. Therefore, another absorbing partner unit in the UV or blue spectral region is needed for colour conversion when combined with an inorganic LED.

For absorption in the blue region and emission in the yellow region, efficient energy transfer between the two partner units needs to occur. One type of energy transfer is the previously described FRET mechanism (see section 10.4.2) where energy is non-radiatively transferred from a donor molecule to an acceptor molecule through dipole-dipole coupling [54]. The efficiency of the energy transfer strongly depends on the spatial separation of the involved molecules. Another possible energy transfer, called Dexter electron transfer, is a quantum mechanical mechanism based on the exchange of an electron between two molecules [72]. Strong overlap of the wave functions of the donor and acceptor molecule is necessary. Both Förster- and Dexter-type energy migrations processes were shown to contribute to the energy transfer in a star-shaped supramolecular from the absorbing truxene core to three emitting BODIPY units [73].

10.5.2.2 Towards white light: Yellow emission from oligofluorene-BODIPY oligomers

The following set of small molecule compounds, four linear oligofluorene-BODIPY structures, are examples illustrating the impact of relatively simple modifications of the chemical structure on the absorption and emission properties [74]. The absorbing partner consists of a chain of either three or four fluorene units. This chain is then coupled with a BODIPY unit at either the *meso*- or *beta*-position as seen in Figure 11(a) and (b), respectively. The unused positions of the BODIPY

unit are blocked with a methyl (Me) or ethyl (Et) group, which also increases the stability of the final molecule. The end products are bright red-orange powders. In solution in toluene or chloroform they are fluorescent under UV irradiation. A full description of the synthesis can be found in Ref. [74].

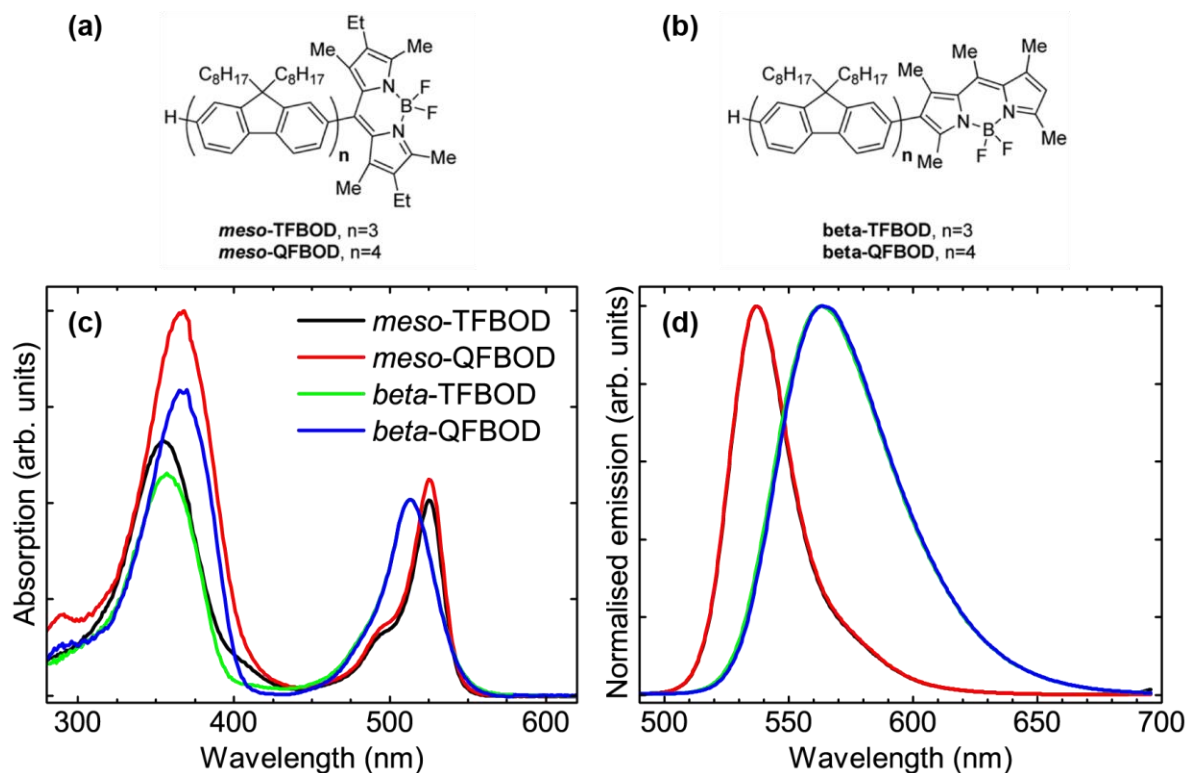


Figure 11 Chemical structure of the linear oligofluorene-BODIPY compounds with the fluorine chain coupled to the (a) meso- and (b) beta-position of BODIPY. (c) UV-vis absorption and (d) normalised PL spectra of the four linear oligofluorene-BODIPY compounds in dichloromethane solution. The excitation wavelength for the PL measurement corresponds to the absorption maximum around 350–370 nm of the oligofluorene chain. Adapted and reprinted with permission from Ref. [74] under Creative Commons License.

UV-vis absorption spectra of all four compounds as a diluted solution in dichloromethane are shown in Figure 11(c). The stronger and shorter wavelength absorption band around 354–370 nm corresponds to the absorption by the oligofluorene chain, whereas the longer wavelength and less intense band around 513–527 nm stems from the BODIPY unit. Extending the conjugation length

from three to four fluorene units results in a redshift of the oligofluorene absorption band by about 12–13 nm for both the *meso*- and *beta*-position. The absorption is also increased by extending the conjugation. Changing the substitution position does not seem to have a large effect on the absorption. The BODIPY absorption band redshifts by about 12 nm when changing the substitution position from *beta* to *meso* for either conjugation length. Figure 11(b) displays PL spectra measured for the four compounds in dilute dichloromethane solutions with an excitation wavelength corresponding to the absorption maximum of the oligofluorene chain. It shows that energy transfer between the oligofluorene chain and the BODIPY unit takes place since the oligofluorene arm is selectively excited while emission from the BODIPY was observed. Changing the substitution position from *meso* to *beta* broadens and redshifts the emission by about 26 nm regardless of the conjugation length of the fluorene chain.

In order to demonstrate the energy down-conversion process, *meso*-QFBOD was deposited from a toluene solution onto a UV LED emitting at around 365 nm. *meso*-QFBOD was chosen as its absorption maximum almost coincides with the emission peak of the UV LED and as it had the strongest absorption band of the four oligofluorene-BODIPY compounds. Optical microscope images of the LED with and without *meso*-QFBOD and under forward bias are displayed in Figure 12(a)–(c), respectively. As seen in the images, a continuous film was not formed, but most of the material has accumulated around and between the two wire contacts of the LED. Figure 12(d) shows the EL spectra of the bare UV LED and the LED coated with *meso*-QFBOD under a forward current of 5 mA. The spectra are normalised to the emission peak of the UV LED around 365 nm in order to see the changes in the emission due to the organic material. Both spectra exhibit a broad emission band peaking just below 600 nm. In the spectrum of the bare UV LED, this weak peak around 585 nm is caused by impurities in the semiconductor material and referred to as yellow

band [75]. In the spectrum of the coated LED, this second emission is much stronger and slightly redshifted to around 590 nm and is due to emission from *meso*-QFBOD. In order to show that the change in the yellow emission band is indeed caused by emission from the organic material the spectrum of the uncoated LED is subtracted from the spectrum of the LED coated with *meso*-QFBOD. Almost no change in the subtracted spectrum is visible indicating that the emission originates from *meso*-QFBOD with negligible contribution from the impurity band. The steeper drop on the shorter wavelength side is due to self-absorption by the second absorption peak of *meso*-QFBOD at 527 nm (see Figure 11(c)).

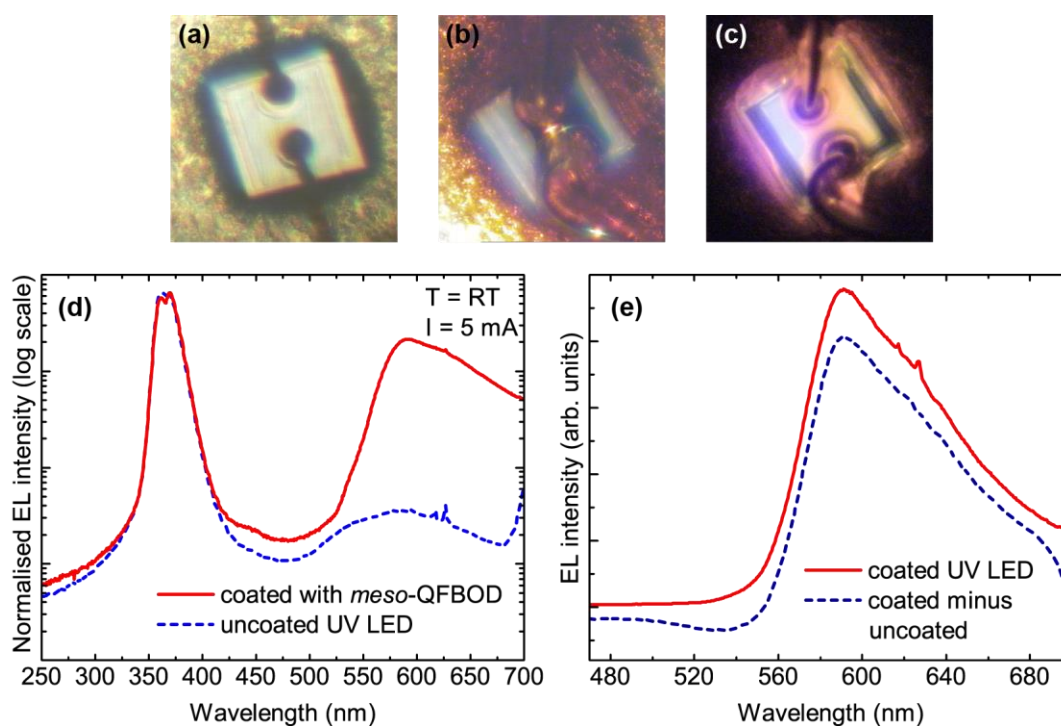


Figure 12 Optical microscope image of the (a) bare UV LED; of the UV LED coated with *meso*-QFBOD (b) switched off and (c) under forward current of 1 mA. The dimension of the LED is $280 \mu\text{m} \times 280 \mu\text{m}$. (d) EL spectra of the uncoated and coated LED under forward current of 5 mA. Both spectra are normalized to the LED emission peak. (e) Spectrum of the uncoated UV LED subtracted from the spectrum of the *meso*-QFBOD coated LED compared with the spectrum of the coated LED in the region of the yellow emission. One $10 \mu\text{l}$ drop (30 mg in 1 ml of solvent) of *meso*-QFBOD was deposited on the LED die. Adapted and reprinted with permission from Ref. [74] under Creative Commons License.

10.5.2.3 Towards white light: Blue light absorption for white LEDs

For white light generation blue light is needed in addition to yellow, which can be achieved by exchanging the absorbing component of the small molecule shown in section 10.5.2.2.

Figure 13(a) displays the chemical structure of (BODFluTh)₂FB and its synthesis is described in Ref. [46]. This compound has the absorbing unit placed in the centre between BODIPY units on either side. The absorbing core consists of a fluorobenzene (FB) at its centre, which is bordered by a thiophene (Th) and a fluorene (Flu) on either side. The fluorene units are substituted at the BODIPY *meso*-position. The hydrocarbon group (C₈H₁₇) on the fluorene units makes the compound soluble. The UV-vis absorption spectrum in Figure 13(b) exhibits an absorption peak around 403 nm corresponding to a charge transfer between the tetrafluorophenylene core and the neighbouring thiophene-fluorene unit and a second absorption peak associated with the absorption of the BODIPY unit. The PL spectrum in Figure 13(b) with a single emission peak at 550 nm shows energy transfer from the core unit to the BODIPY when excited at 440 nm, which is slightly higher than the absorption maximum, but closer to the blue emission needed for white light generation.

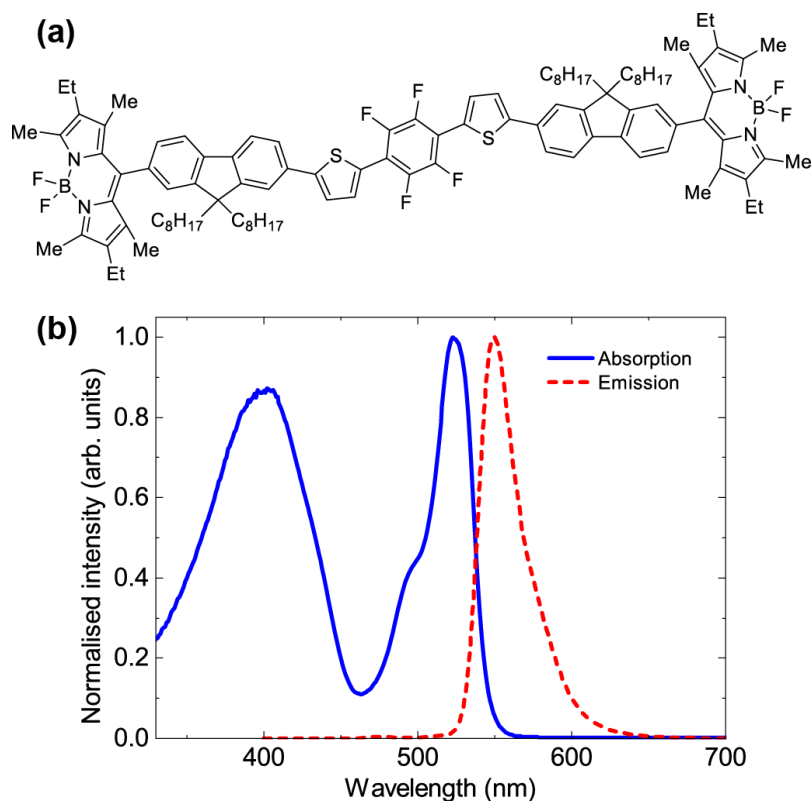


Figure 13 (a) Chemical structure of $(BODFluTh)_2FB$. (b) UV-vis absorption and emission spectra for $(BODFluTh)_2FB$ in dichloromethane solution. The excitation wavelength was 440 nm. Adapted and reprinted with permission from Refs. [29, 46] under Creative Commons License.

10.5.2.4 Towards white light: Nanorod encapsulation

The energy down-conversion process of $(BODFluTh)_2FB$ was studied by applying the organic compound to a GaN-based nanorod structure containing a blue-emitting InGaN/GaN multiple quantum well (MQW) structure ($\lambda \approx 445$ nm) [76]. Details on the used nanorod structure can be found in Ref. [77]. Direct contact of the organic material with the MQW structure should enhance the energy transfer between the blue-emitting nanorods and the converter through FRET mechanism. The converter was drop-casted in solution with toluene (10 mg/1 μ l) on the nanorod structure. Figure 14(a)–(d) displays secondary electron (SE) images recorded using a variable pressure scanning electron microscope from the centre to the edge of the nanorod sample. The film coverage is very non-uniform. At the centre the organic material filled in the gaps between the

nanorods, visible as a semi-transparent haze in Figure 14(b), whereas towards the edge a thick film has formed on top of the nanorods.

The light conversion process was investigated through PL measurements. Since these samples are not complete LED structures (no p-n junction or metal contacts) the emission from the MQW structure embedded in the nanorods was selectively excited using a 405 nm laser. The excitation took place through the polished back surface in order to minimise absorption of the laser light by the organic material on top of the nanorods. PL spectra of the sample with different film thicknesses were recorded by subsequently adding further drops of converter material between the measurements (shown in Figure 14(e)). The emission peak around 446 nm originates from the MQW structure whereas the broad emission above 530 nm is due to down-conversion by the organic material. The steep drop on the shorter wavelength side is due to partial self-absorption of the BODIPY molecule. Overall, the emission intensity from the organic converter material increases with number of deposited drops. However, each additional drop likely leads to dissolution of the existing organic film leading to poor film formation and coverage of the LED with the organic material which impacts the overall colour conversion and emission.

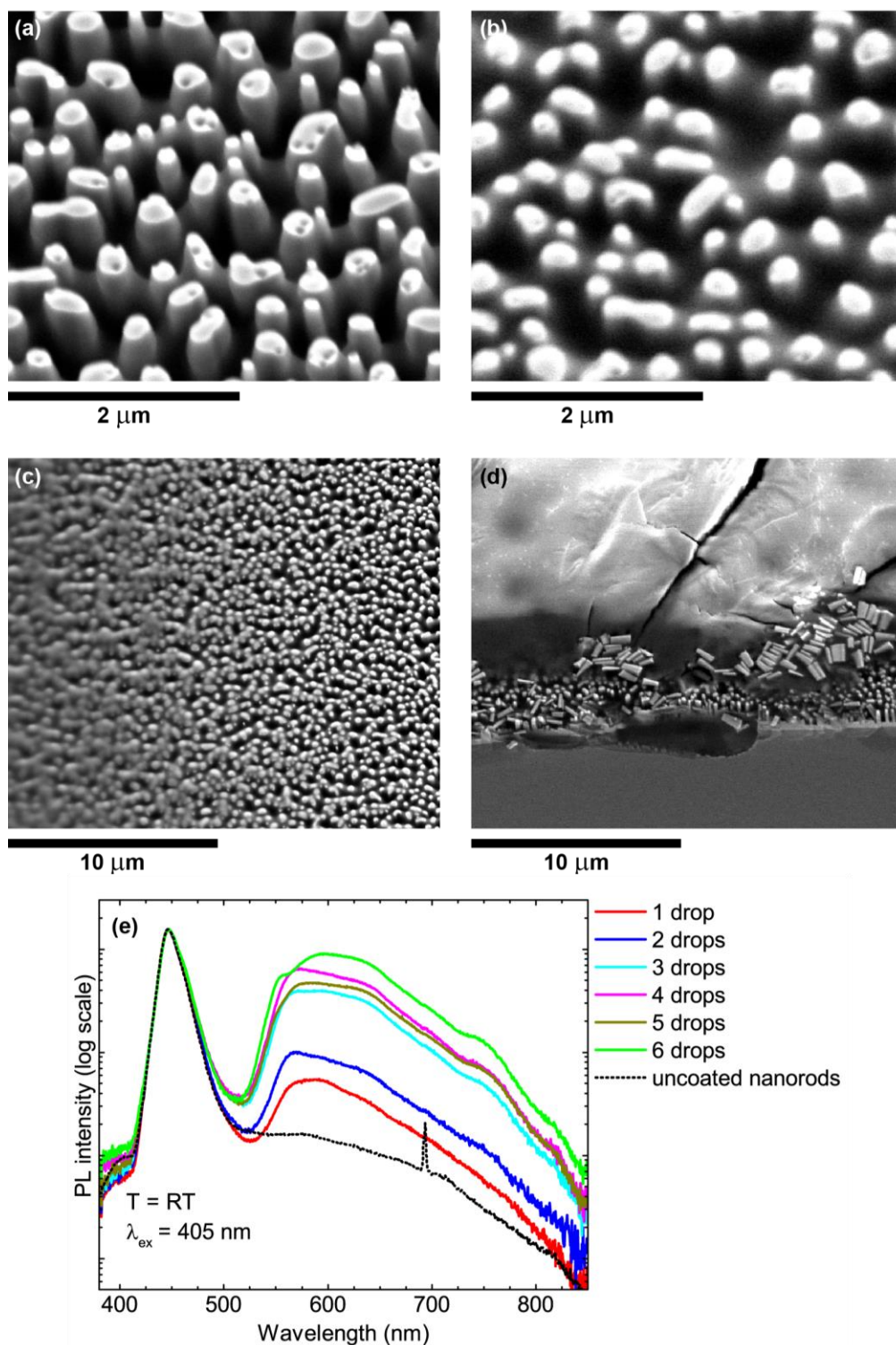


Figure 14 (a)–(d) SE images of nanorods coated with (BODFluTh)₂-FB (in solution with toluene) using a variable pressure SEM (0.5 mbar). The deposited layer exhibits a gradient of increasing thickness towards the sample edge. (e) Normalised PL spectra ($\lambda_{\text{ex}} = 405 \text{ nm}$) of InGaN/GaN MQW nanorod structures coated with (BODFluTh)₂-FB of various film thickness achieved by depositing one to six drops of the organic material. The spectra are normalised to the MQW emission peak of the nanorods. The excitation of the MQW emission using a 405 nm laser was carried out through the back of the sample to minimise absorption of the laser light by the organic material. The InGaN/GaN nanorod structures were fabricated by the group of Prof. Tao Wang at

the University of Sheffield and more details on the structures can be found in Ref. [77]. Modified and reprinted with permission from Ref. [76].

10.5.3 Towards white light: Deposition and encapsulation

The previous two examples use drop-casting as a method of deposition. In both cases the films suffered from strong non-uniformities. In the case of direct deposition on the LED, the small size and the wire bonds were problematic leading to the accumulation of material around the LED edge or wire bonds (Figure 12(a)–(c)). Similar issues were encountered for the nanorod sample with variable film thickness across the sample (Figure 14(a)–(d)). Alternative deposition methods are spin-coating or vacuum deposition, although either could still lead to issues with film formation around the wire bonds. Alternatively, the organic material can be incorporated in a transparent, non-emissive matrix to encapsulate the entire LED chip [78]. Advantages of this encapsulation method are that only small concentrations of the colour converter are required, the solution emission properties are retained, and rapid curing can be achieved using UV light.

Therefore, the organic material, (BODFluTh)₂FB, was dissolved in 1,4-cyclohexanedimethanol divinyl ether (CHDV) containing trace amounts of the photoacid generator (PAG) 4-octyloxy diphenyliodonium hexafluoroantimonate at concentrations of 0.25–4% weight per volume (w/v) [29]. The solution was drop-cast onto the blue LED chip filling the cup with the LED die and cured using UV light to harden the encapsulant. Optical microscope images of the hybrid LEDs are shown in Figure 15(a) where the organic material becomes orange from pale yellow with increasing concentration. The SE images in Figure 15(b) show that the LED is fully encapsulated and a dome has formed over the LED chip.

EL spectra of the hybrid LEDs under a continuous forward current of 25 mA using different concentrations are displayed in Figure 15(c). With increasing converter concentration, both the intensity of the blue LED and of the yellow organic emission decrease. Overall, however, the

intensity of the yellow emission increases with respect to the blue intensity. This causes the emission colour to shift from blue-ish to white and then into the yellow-orange as seen in the chromaticity diagram in Figure 15(d) by an almost linear shift with concentration. The simultaneous decrease of both emission peaks implies that with increasing concentration more blue light is getting absorbed but not re-emitted as yellow. This quenching effect is caused by aggregation of the organic molecules within the encapsulant with increasing concentration due to their close proximity leading to non-radiative recombination [46, 79]. Similarly, this aggregation also causes a redshift of the organic emission with increasing concentration which leads to the slight deviation of the straight line at higher concentrations in the chromaticity diagram [80].

By controlling the concentration of the colour converter, (BODFluTh)₂FB, in the encapsulant and the volume of the deposited drop it is possible to produce warm and cool white light emission. The warm hybrid LED has a CCT of 2770 K, and CRI of 20 and chromaticity coordinates (0.45, 0.41), whereas the cool LED possesses a CCT of 7680 K, CRI of 46 and chromaticity coordinates (0.31, 0.27) [29]. As a reference, pure white is located at (0.33, 0.33). It should be noted that both LEDs exhibit poor colour rendering due to the absence of emission in the green spectral range, where the human eye is most sensitive. The lack of green emission is further enhanced due to self-absorption of BODIPY.

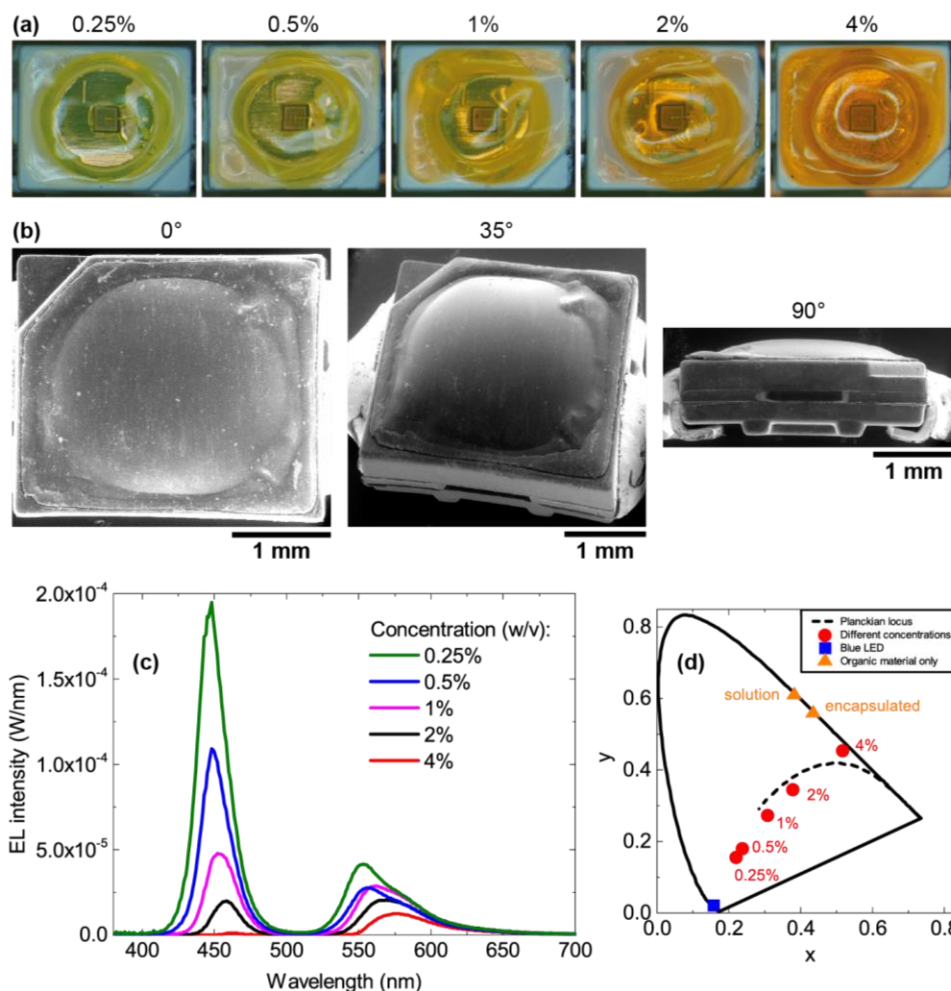


Figure 15 (a) Optical microscope images of the hybrid LEDs using concentrations of 0.25-4% w/v of the colour converter (BODFluTh):FB. (b) SE images of one of the hybrid LEDs at different viewing angles. (c) EL spectra of the same hybrid LEDs operated under a continuous forward current of 25 mA. (d) CIE1931 chromaticity diagram showing the location of the hybrid LED with respect to the Planckian locus. The coordinates of the bare blue LED and the organic material in solution and encapsulated state are also shown. Adapted and reprinted with permission from Ref. [29] under Creative Commons License.

10.5.4 White light device efficiency and efficacy

The “efficiency” of the device and the organic colour converter can be assessed by different parameters, as defined in section 10.2.2.

The efficiency of energy-down converting materials is commonly described by the photoluminescence quantum yield (PLQY), which is the ratio of emitted and absorbed photons. It is generally determined using an integrating sphere system and only describes the efficiency of the material itself. An example of a double integrating sphere system used to measure the PLQY is

given in Ref. [81], which allows the differentiation of reflected and transmitted light through the sample which is placed between the two spheres.

For (BODFluTh)₂FB the PLQY was determined in solution (dichloromethane) and in the encapsulated state and estimated to be 60% and 63%, respectively [46], confirming that the transparent matrix has a negligible impact on the optical properties.

The quantum conversion efficiency of (BODFluTh)₂FB when applied to the blue LED in the encapsulant is also measured and fully described in Ref. [29] using a similar methodology as Ref. [81]. It is given by the ratio of the number of converted photons (yellow emission from the organic material) and the number of absorbed photons from the blue LED. It is only an estimation since only the entire emitted light is measured using a single integrating sphere. Neither transmitted nor reflected light can be differentiated, or light that is trapped in the LED package. However, it still is an estimation of the efficiency when combined directly with an LED. The conversion efficiency of different concentrations of (BODFluTh)₂FB in the encapsulant applied to a blue LED is shown in Figure 16. It decreases with increasing concentration due to aggregation induced luminescence quenching. The conversion efficiency of 62% at the lowest concentration (0.25% w/v) is in agreement with the PLQY indicating low aggregation at that concentration.

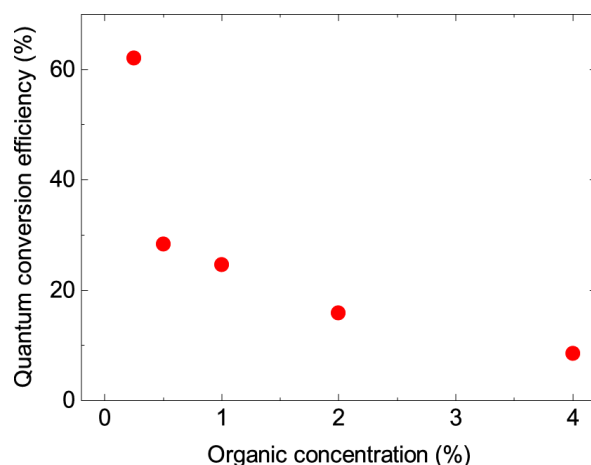


Figure 16 Quantum conversion efficiency of (BODFluTh)₂FB applied to a blue LED as a function of concentration in the encapsulant. Reprinted with permission from Ref. [29] under Creative Commons License.

Commonly, the luminous efficacy (of a light source) is given to provide a number for efficiency. The warm and cool white LED from the previous section have luminous efficacies of 3 lm/W and 11 lm/W, respectively. Alternatively, the efficiency of white LEDs can also be described by the blue-to-white (B-W) efficacy as defined in section 10.2.2. The warm hybrid LED (4% w/v (BODFluTh)₂FB)) has a B-W efficacy of 29 lm/W, whereas the efficacy of the cool LED (1% w/v (BODFluTh)₂FB) is 96 lm/W. Phosphor-based white LEDs have B-W efficacies above 200 lm/W. The difference in efficacy between those two LEDs is due to the aggregation-induced luminescence quenching, while the low efficacies of the (BODFluTh)₂FB hybrid LEDs are predominantly caused by the lack of green emission where the human eye is most sensitive (since the luminous efficacy is directly proportional to the luminous flux).

10.5.5 White light degradation and lifetime

For real applications the lifetime of the hybrid devices and hence organic colour converters is crucial. For this purpose, degradation studies of the hybrid LEDs coated with (BODFluTh)₂FB were performed [29, 46]. In an initial experiment the hybrid LED was measured periodically for a month, but only operated for the duration of the measurement (around 5 s). Negligible changes in emission characteristics, chromaticity coordinates or CCT were observed. Therefore, the experiment was repeated, but with continuous operation of the LED. After 7 hours the luminous efficacy dropped below 60% of its initial value as seen in Figure 17(a). The emission from the organic material decreased drastically, while the blue LED emission remained constant indicating that the absorbed blue light is not reemitted in the spectral region. In order to investigate if the heat

generated by the LED causes this degradation, the (BODFluTh)₂FB encapsulant was deposited on a transparent glass slide and placed 5 mm above the LED. Again, the LED was continuously operated up to 750 hours (31 days) and spectra recorded at different time intervals. The luminous efficacy is shown in Figure 17(a) together with the results from the LED where the material is directly applied to the LED. The values are normalised to the initial value for comparison. After about 200 hours the luminous efficacy decreased by less than 10%, while almost no change was observed for the CCT or chromaticity coordinates. Even after one month of continuous operation the luminous efficacy only decreased by 15%. The chromaticity coordinates shifted from (0.36, 0.32) to (0.32, 0.28) and the CCT from 4400 K to 6500 K. Similar continuous operation studies were carried out for the blue LED coated with only the transparent encapsulant (CHDV with PAG). The results showed that the transparent encapsulant was not affected by the LED or temperature over time indicating it is optically stable during operation of the LED.

The same (BODFluTh)₂FB encapsulated LED was also remeasured after 15 months using a pulsed current to minimise heating of the LED [29]. The initially recorded EL spectrum and spectrum after 15 months is displayed in Figure 17(b). The decrease in intensity from the organic material in the transparent matrix indicates degradation due to oxygen and/or moisture in the environment. The LED emission was stable over time. Figure 17(b) also shows the spectra of the same LED measured using either continuous or pulsed current conditions. It can be observed that the yellow emission intensity is higher for pulsed current operation compared with continuous current, while the blue LED emission remains the same. Time-resolved luminescence measurements showed that both the blue LED and the organic material have similar decay times in the order of 10s of nanoseconds ruling out different decay times as the cause for the observed differences in intensity. It is more likely that increased population of non-radiative triplet states during continuous current

operation is the cause of a drop in intensity [82]. During pulsed current operation the ground state can be populated again since the triplet lifetime (up to 100 μs) is shorter than the pulse period of the current pulse of 500 μs [83].

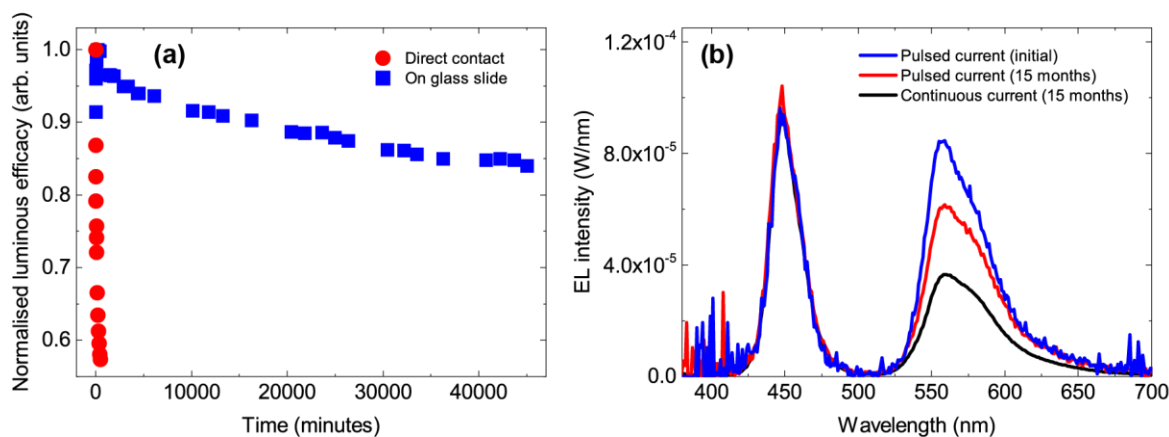


Figure 17 (a) Normalised luminous efficacy of a hybrid LED with the (BODFluTh)₂FB encapsulant directly applied to the LED or on a glass slide 5 mm above the blue LED. The data shown here is the same as in figures S6 and S8 of Ref. [46] except that the LED with the material applied on a glass slide was operated for longer since publication. (b) EL spectra of the same hybrid LED measured using pulsed and continuous current of 25 mA and remeasured after 15 months. Modified and reprinted with permission from Refs. [29, 46] under Creative Commons License.

10.5.5 Next generation white-emitting LEDs with improved efficacy

An alternative approach to small molecule colour converters focused on removing the BODIPY emissive unit to eliminate the inherent self-absorption at green wavelengths, thereby increasing the colour rendering and efficiency (see section 10.2.2).

Two compounds bearing either one or two units of benzothiadiazole (BT) coupled to fluorene and peripheral triphenylamine donor units, (TPA-Flu)₂BT and (TPA-Flu)₂BTBT, as shown in Figure 18(a) and (b), respectively, were reported [84]. As seen in the UV-vis absorption and emission spectra in Figure 18(c), the two absorption peaks at 345 nm and 430/443 nm of both compounds marginally overlap with their emission peaks at 570/584 nm. Introduction of the second BT unit redshifts both the second absorption peak and the emission by 13 nm and 14 nm, respectively.

In order to investigate the down-conversion properties the compounds were incorporated into a transparent encapsulant (CHDV with PAG) and deposited on blue LEDs. Example EL spectra of different concentrations of the two compounds yielding warm and cool white light are shown in Figure 18(d). For comparison, the spectrum of a (BODFluTh)₂FB hybrid LED is included as well showing that the two new compounds exhibit a much broader emission from the organic material in the green to yellow spectral range. This is reflected by the much higher CRI of 51–66 for the single BT compound and 40–61 for the double BT compound depending on the concentration showing that reasonable colour rendering can be achieved. The chromaticity coordinates of the entire concentration series are shown in Figure 18(e) with the points corresponding to the warm and cool LEDs marked by circles. As before, changing the concentration shifts the chromaticity coordinates along a straight line from the blue to the yellow/green region in the chromaticity diagram.

Luminous efficacies of 41 lm/W and 10 lm/W, and B-W efficacies of 368 lm/W and 116 lm/W for (TPA-Flu)₂BT and (TPA-Flu)₂BTBT, respectively, were reported. The much lower efficacies of (TPA-Flu)₂BTBT are due to the low PLQY of 17% compared with the 63% for (TPA-Flu)₂BT. The much higher efficacy numbers for the (TPA-Flu)₂BT LEDs compared with (BODFluTh)₂FB (luminous and B-W efficacies: 13.6 lm/W and 100–120 lm/W [29, 46]) are due to the enhanced green emission in the 490–520 spectral range. The B-W efficacy also exceeds the values of phosphor-based white LEDs (200–300 lm/W). It should be noted that these numbers are comparable because the blue LEDs used in these studies were the identical for all measurements.

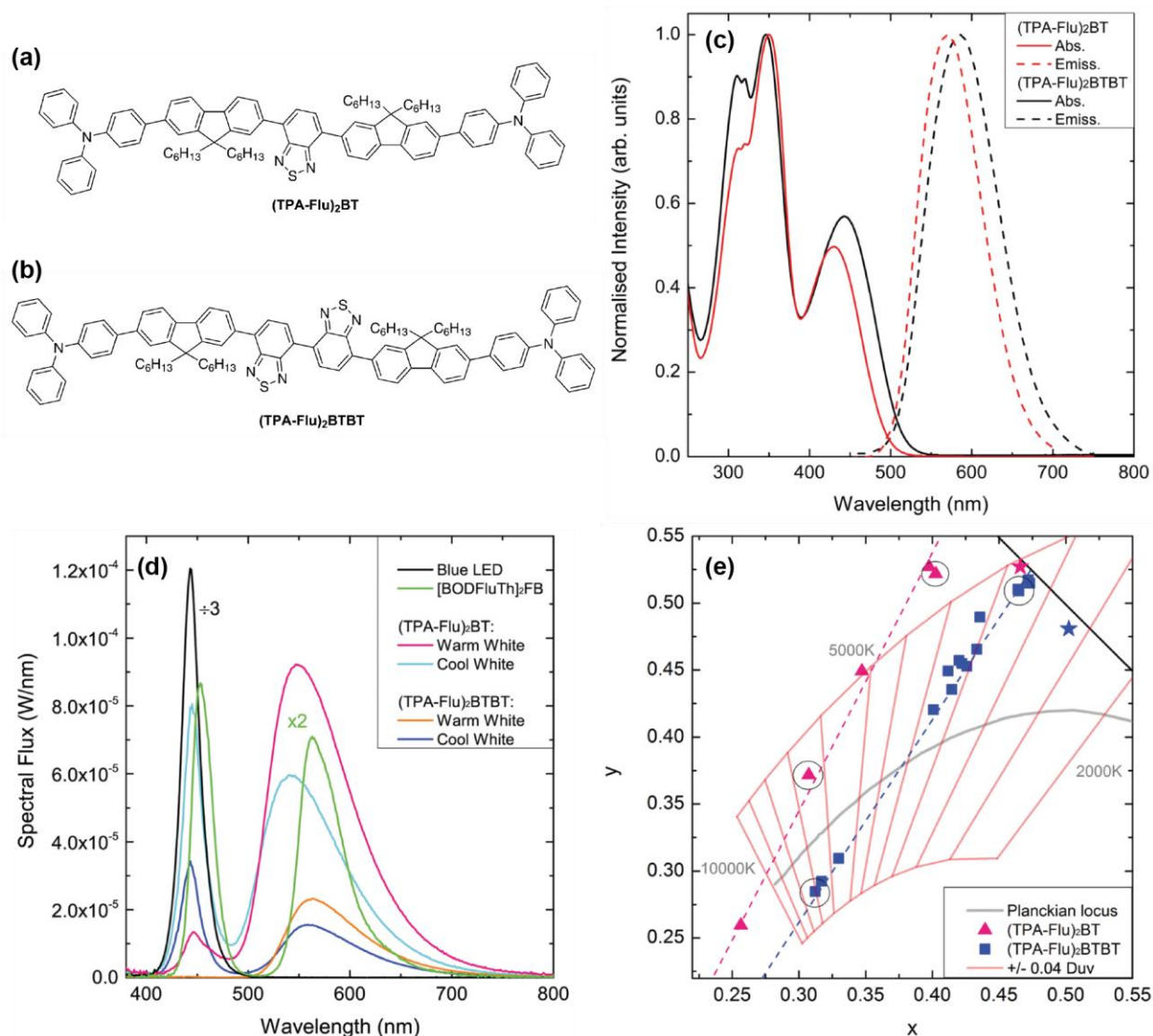


Figure 18 Chemical structure of (a) (TPA-Flu)₂BT and (b) (TPA-Flu)₂BTBT. (c) Normalised UV-vis absorption and emission spectra of both compounds in dichloromethane dilute solution. (d) Example EL spectra of the (TPA-Flu)₂BT and (TPA-Flu)₂BTBT hybrid LEDs demonstrating warm and cool white light emission. For comparison the spectrum for a (BODFluTh)₂FB LED is shown. (e) 1931 CIE chromaticity diagram showing the chromaticity coordinates for both compounds as an evolution of concentration. The circled data points correspond to the warm and cool LEDs from (d). Adapted and reprinted with permission from Ref. [84] under Creative Commons License.

10.5.6 Metal-organic frameworks (MOFs)

One issue encountered with previous colour converters is aggregation of the molecules with increasing concentration. This aggregation can impact optical properties by redshifting and quenching the luminescence due to non-radiative recombination [29, 46, 79].

One method to counteract this is to integrate small molecule emissive compounds into a metal-organic framework (MOF), which are well-defined rigid networks where the organic material, or ligand, is connected through metal ions to the network. This integration into a rigid network should prevent aggregation and preserve or improve the optical properties as schematically shown in Figure 19(a) [85, 86].

The structure of the benzothiadiazole-based organic compound BTBMBA is shown in Figure 19(b) [87]. To synthesise the MOF structure MOF-MTBMBA, the ligand BTBMBA was linked by Zr ions to form a structure with UiO-68 topology (Figure 19(c)) [88, 89]. The SE image of MOF-MTBMBA in Figure 19(d) shows the regular octahedral morphology of the crystals with sizes around 500–700 nm.

To investigate the optical properties, the material was incorporated into a commercially available polyurethane resin, OptiTEC™ 4200. The UV-vis absorption and emission spectra of the free ligand and the ligand incorporated into the MOF structure are shown in Figure 19(e). Both have a single absorption peak at 408 and 412 nm and emission peak at 501 and 514 nm for MTBMBA and MOF-MTBMBA, respectively. The slight blueshift for the MOF structure for both absorption and emission, is associated with the steric confinement of the ligand in the MOF causing an altered environment of the ligand.

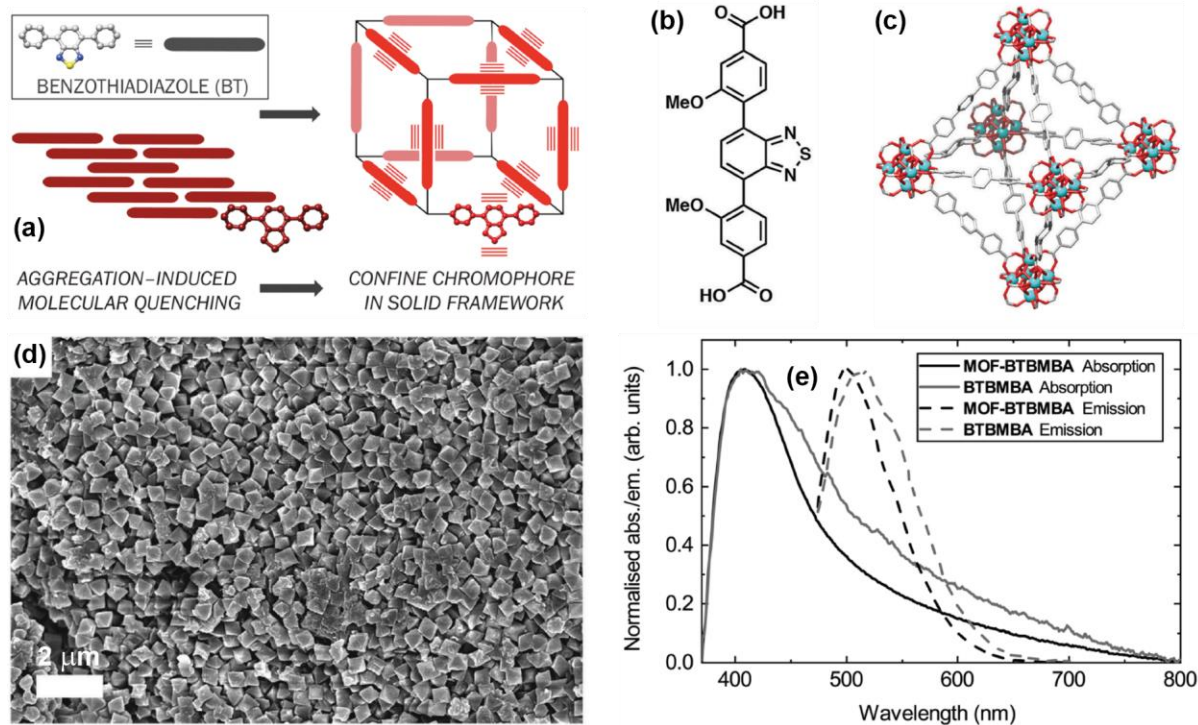


Figure 19 (a) Schematic of aggregation-induced luminescence quenching and integration into MOF structure. (b) Structure of BTB MBA. (c) Crystal structure of UiO-68 used for MOF-BTB MBA. (d) SE image of MOF-BTB MBA. (e) UV-vis absorption and emission of BTB MBA and MOF-BTB MBA encapsulated in the polyurethane resin. Adapted and reprinted with permission from Ref. [87] under Creative Commons License.

A series of hybrid LEDs were prepared using different concentrations (0.33–4%) of the ligand (BTB MBA) or the MOF (MOF-BTB MBA) incorporated into the resin. The EL spectra on identical logarithmic intensity scales of those two concentrations series are shown in Figure 20(a) and (b). Although weak both exhibit an emission peak around 550 nm, which is increasing with concentration, in addition to the emission from the blue LED. The spectra of the bare blue LEDs before they were coated with the converter materials do not have this emission peak, clearly indicating energy conversion into the yellow region by the organic material. Most noteworthy is the increased intensity for the MOF-BTB MBA LEDs compared with the free ligand LEDs as displayed in Figure 20(c), which shows the ratio of the integrated emission intensities of the coated LED and the bare blue LEDs in the wavelength range of 525–600 nm.

To further investigate this observation, the luminous efficacy was determined for both hybrid LED series and is shown in Figure 20(d). It increases with increasing concentration for the LEDs coated with the MOF structure, whereas the free ligand versions show a decrease in efficacy. This is caused by the luminous flux which shows the same behaviour. This indicates that with increasing concentration the ligand keeps absorbing the blue light but does not transfer and re-emit it at longer wavelength. On the other hand, the MOF structure shows the opposite behaviour. This is most likely caused by luminescence quenching due to aggregation of the free ligand. Incorporation into the MOF structure enhances the light emission by suppressing aggregation. While the device properties are far from outstanding, this showcases the promise of this methodology as a means to fabricate hybrid LEDs using MOFs.

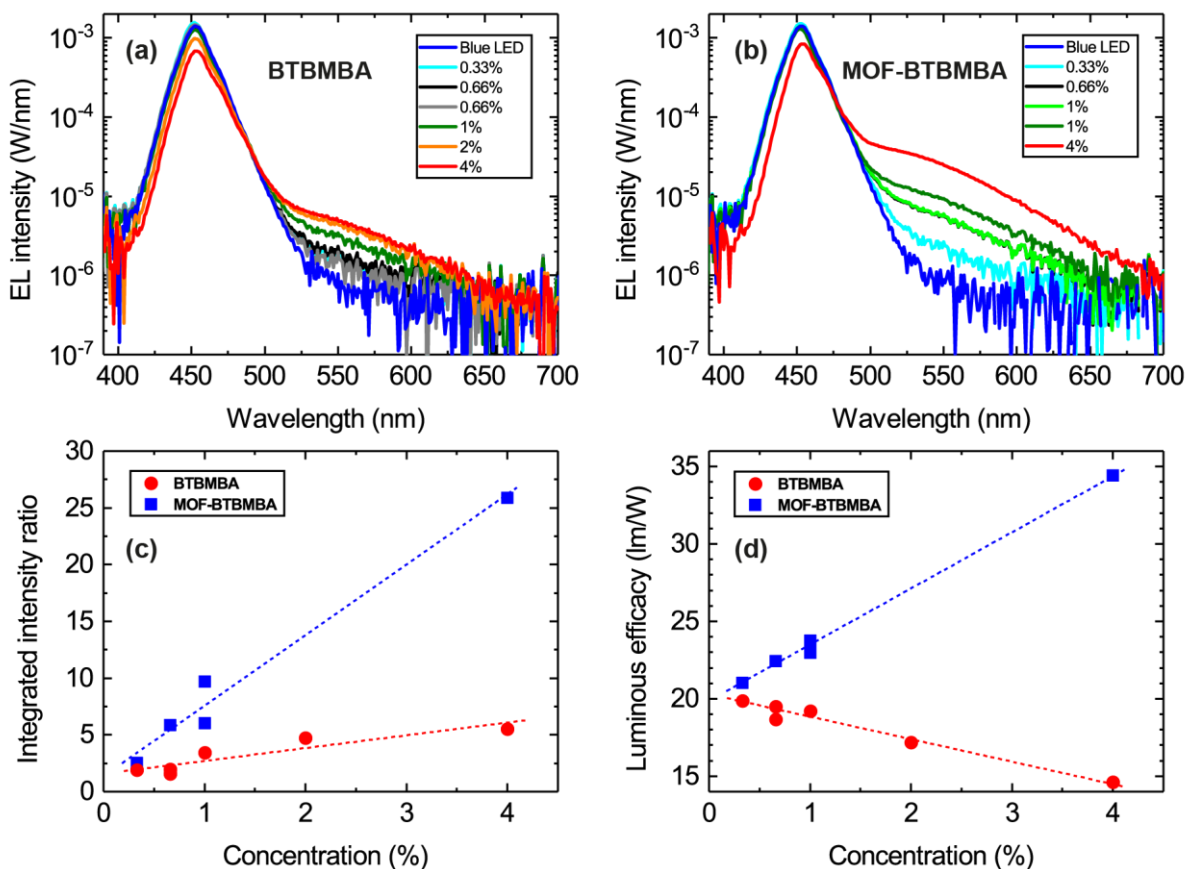


Figure 20 EL spectra of the blue LEDs coated with the (a) ligand BTMBA and (b) MOF-BTMBA using concentrations of 0.33–4% in the polyurethane resin. (c) Ratio of the integrated intensities of the coated LEDs and the bare blue LEDs in the wavelength range of 525–600 nm and (d) luminous efficacies of the two hybrid LED series. Adapted and reprinted with permission from Ref. [87] under Creative Commons License.

10.6 Summary

This chapter has illustrated the functionality of hybrid inorganic-organic LEDs. This technology utilises the high efficiency of blue inorganic LEDs and combines it with the versatility of organic colour converters to provide an alternative method for white light generation.

The extended background was aimed to provide a sufficient introduction to nitride semiconductors and their LEDs, but also to familiarise the reader with the background to colorimetry and radiometry of light sources. For example, the terms efficiency and efficacy are related, but can describe quite different properties. It is also important, to consider what factors contribute to these colour parameters, e.g. luminous efficacy and CRI, in order to know what properties of the colour converter need to be adjusted or modified for the desired emission characteristics.

A brief introduction and background to the chemistry behind organic colour converting compounds aimed to showcase the number of factors that can be controlled and modified when designing organic colour converters. Although not comprehensive, it hopefully provided some context for the latter two sections.

Light-emitting polymers are one choice of organic colour converter. They are readily commercially available and cost effective. The examples given, demonstrate their colour conversion capabilities using either one or multiple polymers or polymers in combination with other types of colour converters.

Luminescent small molecules have the advantage of a precisely known molecular structure which allows straightforward replication. Their absorption and emission can also be easily tuned through the manipulation of their structure, such as exchanging units or changing the conjugation length,

to achieve the desired colour characteristics. This section presented examples that demonstrate the evolution of a series of novel small molecule-based converters to adjust and improve their colour conversion properties when coupled with a blue inorganic LED. It highlighted the design considerations and changes made to the small molecule in order to achieved the desired white light emission. Before applying to the inorganic LED, the deposition method needs to be considered in order to achieve good coverage of the LED chip but also, for example, prevent detrimental aggregation-induced effects on the luminescence. Remaining challenges, such as lifetime and degradation, which are needed to make small molecules commercially viable, were also discussed.

Acknowledgements

The research carried out by the authors was funded by the UK Engineering and Physical Sciences Research Council (EPSRC).

References

1. Shchekin, O. and M.G. Craford, *History of Solid-State Light Sources*, in *Handbook of Advanced Lighting Technology*, R. Karlicek, et al., Editors. 2017, Springer International Publishing: Cham. p. 1-30.
2. Zukauskas, A., M.S. Shur, and R. Gaska, *Introduction to Solid-State Lighting*. 2002: Wiley-Interscience.
3. *Introduction to Nitride Semiconductor Blue Lasers and Light Emitting Diodes*, ed. S. Nakamura and S.F. Chichibu. 2000: CRC Press
4. Available from: <https://www.nobelprize.org/prizes/physics/2014>.
5. Schubert, E.F., *Light-Emitting Diodes*. 2006: Cambridge University Press.
6. McKittrick, J. and L.E. Shea-Rohwer, *Review: Down Conversion Materials for Solid-State Lighting*. *Journal of the American Ceramic Society*, 2014. **97**(5): p. 1327-1352.
7. Massari, S. and M. Ruberti, *Rare earth elements as critical raw materials: Focus on international markets and future strategies*. *Resources Policy*, 2013. **38**(1): p. 36-43.
8. Kamtekar, K.T., A.P. Monkman, and M.R. Bryce, *Recent Advances in White Organic Light-Emitting Materials and Devices (WOLEDs)*. *Advanced Materials*, 2010. **22**(5): p. 572-582.
9. Farinola, G.M. and R. Ragni, *Organic emitters for solid state lighting*. *Journal of Solid State Lighting*, 2015. **2:9**(1).

10. *III-Nitride Based Light Emitting Diodes and Applications*, ed. T.-Y. Seong, et al. 2013: Springer Netherlands.
11. *III-Nitride Ultraviolet Emitters: Technology and Applications*, ed. M. Kneissl and J. Rass. 2016: Springer International Publishing.
12. Gorczyca, I., et al., *Limitations to band gap tuning in nitride semiconductor alloys*. Applied Physics Letters, 2010. **96**(10): p. 101907.
13. Morkoç, H., *Handbook of Nitride Semiconductors and Devices: Materials Properties, Physics and Growth, Volume 1*. 2008: WILEY-VCH.
14. Neamen, D., *Semiconductor Physics And Devices*. 4 ed. 2011: McGraw-Hill Education.
15. Chichibu, S., K. Wada, and S. Nakamura, *Spatially resolved cathodoluminescence spectra of InGaN quantum wells*. Applied Physics Letters, 1997. **71**(16): p. 2346-2348.
16. Sugahara, T., et al., *Direct Evidence that Dislocations are Non-Radiative Recombination Centers in GaN*. Japanese Journal of Applied Physics, 1998. **37**(Part 2, No. 4A): p. L398-L400.
17. Casey, H.C., B.I. Miller, and E. Pinkas, *Variation of minority-carrier diffusion length with carrier concentration in GaAs liquid-phase epitaxial layers*. Journal of Applied Physics, 1973. **44**(3): p. 1281-1287.
18. Ettenberg, M., H. Kressel, and S.L. Gilbert, *Minority carrier diffusion length and recombination lifetime in GaAs:Ge prepared by liquid-phase epitaxy*. Journal of Applied Physics, 1973. **44**(2): p. 827-831.
19. *Commission internationale de l'Eclairage Proceedings*. 1931.
20. Vos, J.J., *Colorimetric and photometric properties of a 2° fundamental observer*. Color Research & Application, 1978. **3**(3): p. 125-128.
21. MacAdam, D.L., *Specification of small chromaticity differences*. J. Opt. Soc. Am., 1943. **33**(1): p. 18-26.
22. Wyszecki, G. and W.S. Stiles, *Color Science: Concepts and Methods, Quantitative Data and Formulae*. 2 ed. 2000: Wiley-Blackwell.
23. Planck, M., *Ueber eine Verbesserung der Wien'schen Spectralgleichung*. Verhandlungen der Deutschen physikalischen Gesellschaft, 1900. **13**: p. 202-202.
24. Planck, M., *Ueber das Gesetz der Energieverteilung im Normalspectrum*. Ann. Phys., 1901. **309**(3): p. 553-563.
25. Wien, W., *Ueber die Energievertheilung im Emissionsspectrum eines schwarzen Körpers*. Anal. Phys., 1896. **294**: p. 662-662.
26. in *CIE No. 17.4: International lighting vocabulary*. 1987.
27. Taylor, E., P.R. Edwards, and R.W. Martin, *Colorimetry and efficiency of white LEDs: Spectral width dependence*. physica status solidi (a), 2012. **209**(3): p. 461-464.
28. in *CIE No. 13.3: Method of measuring and specifying colour rendering properties of light sources*. 1995.
29. Bruckbauer, J., et al., *Colour tuning in white hybrid inorganic/organic light-emitting diodes*. Journal of Physics D: Applied Physics, 2016. **49**(40): p. 405103-405103.
30. Bando, K., et al., *Development of High-bright and Pure-white LED Lamps*. J. Light & Vis. Env., 1998. **22**(1): p. 2-5.
31. Schlotter, P., et al., *Fabrication and characterization of GaN/InGaN/AlGaIn double heterostructure LEDs and their application in luminescence conversion LEDs*. Mater. Sci. Eng. B, 1999. **59**(1): p. 390-394.
32. Ronda, C.R., T. Jüstel, and H. Nikol, *Rare earth phosphors: fundamentals and*

- applications*. J. Alloys Compd., 1998. **275**(0): p. 669-676.
33. *Organic Light Emitting Devices: Synthesis, Properties and Applications*, ed. K. Müllen and U. Scherf. 2006: Wiley-VCH.
 34. Reineke, S., et al., *White organic light-emitting diodes: Status and perspective*. Reviews of Modern Physics, 2013. **85**(3): p. 1245-1293.
 35. Cho, Y.J., K.S. Yook, and J.Y. Lee, *Cool and warm hybrid white organic light-emitting diode with blue delayed fluorescent emitter both as blue emitter and triplet host*. Scientific Reports, 2015. **5**(1): p. 7859.
 36. Yu, L., et al., *Red, Green, and Blue Light-Emitting Polyfluorenes Containing a Dibenzothiophene-S,S-Dioxide Unit and Efficient High-Color-Rendering-Index White-Light-Emitting Diodes Made Therefrom*. Advanced Functional Materials, 2013. **23**(35): p. 4366-4376.
 37. Kim, T.H., et al., *White-Light-Emitting Diodes Based on Iridium Complexes via Efficient Energy Transfer from a Conjugated Polymer*. Advanced Functional Materials, 2006. **16**(5): p. 611-617.
 38. Angioni, E., et al., *A single emitting layer white OLED based on exciplex interface emission*. J. Mater. Chem. C, 2016. **4**: p. 3851-3856.
 39. Roncali, J., *Synthetic Principles for Bandgap Control in Linear π -Conjugated Systems*. Chemical Reviews, 1997. **97**(1): p. 173-206.
 40. Roncali, J., *Molecular Engineering of the Band Gap of π -Conjugated Systems: Facing Technological Applications*. Macromolecular Rapid Communications, 2007. **28**(17): p. 1761-1775.
 41. Bredas, J.-L., *Mind the gap!* Materials Horizons, 2014. **1**(1): p. 17-19.
 42. Schlotter, P., R. Schmidt, and J. Schneider, *Luminescence conversion of blue light emitting diodes*. Appl. Phys. A, 1997. **64**(4): p. 417-418.
 43. Hide, F., et al., *White light from InGaN/conjugated polymer hybrid light-emitting diodes*. Applied Physics Letters, 1997. **70**(20): p. 2664-2666.
 44. Zhang, C. and A.J. Heeger, *Gallium nitride/conjugated polymer hybrid light emitting diodes: Performance and lifetime*. Journal of Applied Physics, 1998. **84**(3): p. 1579-1582.
 45. Gather, M.C., A. Köhnen, and K. Meerholz, *White Organic Light-Emitting Diodes*. Advanced Materials, 2011. **23**(2): p. 233-248.
 46. Findlay, N.J., et al., *An Organic Down-Converting Material for White-Light Emission from Hybrid LEDs*. Advanced Materials, 2014. **26**: p. 7290-7290.
 47. Kanibolotsky, A.L., I.F. Perepichka, and P.J. Skabara, *Star-shaped pi-conjugated oligomers and their applications in organic electronics and photonics*. Chem. Soc. Rev., 2010. **39**: p. 2695-2728.
 48. *Organic Light-Emitting Materials and Devices* ed. Z.R. Li. 2015: CRC Press
 49. *Organic Light-Emitting Devices*, ed. J. Shinar. Springer.
 50. Bernius, M.T., et al., *Progress with Light-Emitting Polymers*. Advanced Materials, 2000. **12**(23): p. 1737-1750.
 51. Ying, L., et al., *White Polymer Light-Emitting Devices for Solid-State Lighting: Materials, Devices, and Recent Progress*. Advanced Materials, 2014. **26**(16): p. 2459-2473.
 52. Smith, R., et al., *Hybrid III-Nitride/Organic Semiconductor Nanostructure with High Efficiency Nonradiative Energy Transfer for White Light Emitters*. Nano Letters, 2013. **13**(7): p. 3042-3047.
 53. Baldo, M.A., et al., *Highly efficient phosphorescent emission from organic*

- electroluminescent devices*. Nature, 1998. **395**(6698): p. 151-154.
54. Förster, T., *Zwischenmolekulare Energiewanderung und Fluoreszenz*. Ann. Phys., 1948. **437**(1-2): p. 55-75.
 55. Achermann, M., et al., *Energy-transfer pumping of semiconductor nanocrystals using an epitaxial quantum well*. Nature, 2004. **429**: p. 642-642.
 56. Jiang, H.X. and J.Y. Lin, *Nitride micro-LEDs and beyond - a decade progress review*. Optics Express, 2013. **21**(S3): p. A475-A484.
 57. Rajbhandari, S., et al., *A review of gallium nitride LEDs for multi-gigabit-per-second visible light data communications*. Semiconductor Science and Technology, 2017. **32**(2): p. 023001.
 58. Lin, J.Y. and H.X. Jiang, *Development of microLED*. Applied Physics Letters, 2020. **116**(10): p. 100502.
 59. Heliotis, G., et al., *Spectral conversion of InGaN ultraviolet microarray light-emitting diodes using fluorene-based red-, green-, blue-, and white-light-emitting polymer overlayer films*. Applied Physics Letters, 2005. **87**(10): p. 103505-103505.
 60. Chun, H., et al., *Visible Light Communication Using a Blue GaN μ LED and Fluorescent Polymer Color Converter*. IEEE Photonics Technology Letters, 2014. **26**(20): p. 2035-2038.
 61. O'Brien, D.C., et al. *Visible light communications: Challenges and possibilities*. in *2008 IEEE 19th International Symposium on Personal, Indoor and Mobile Radio Communications*. 2008.
 62. Chen, M., et al., *Application of a novel red-emitting cationic iridium(III) coordination polymer in warm white light-emitting diodes*. Optical Materials, 2018. **76**: p. 141-146.
 63. Jang, E., et al., *White-Light-Emitting Diodes with Quantum Dot Color Converters for Display Backlights*. Advanced Materials, 2010. **22**(28): p. 3076-3080.
 64. Mangum, B.D., et al., *Exploring the bounds of narrow-band quantum dot downconverted LEDs*. Photonics Research, 2017. **5**(2): p. A13-A22.
 65. Volkan Demir, H., et al., *White light generation tuned by dual hybridization of nanocrystals and conjugated polymers*. New Journal of Physics, 2007. **9**(10): p. 362-362.
 66. Ulrich, G., R. Ziessel, and A. Harriman, *The Chemistry of Fluorescent Bodipy Dyes: Versatility Unsurpassed*. Angew. Chem. Int. Ed., 2008. **47**(7): p. 1184-1201.
 67. Ikawa, Y., S. Moriyama, and H. Furuta, *Facile syntheses of BODIPY derivatives for fluorescent labeling of the 3' and 5' ends of RNAs*. Anal. Biochem., 2008. **378**(2): p. 166-170.
 68. Bonardi, L., et al., *Fine-Tuning of Yellow or Red Photo- and Electroluminescence of Functional Difluoro-boradiazaindacene Films*. Advanced Functional Materials, 2008. **18**(3): p. 401-413.
 69. Hattori, S., et al., *Charge Separation in a Nonfluorescent Donor-Acceptor Dyad Derived from Boron Dipyrromethene Dye, Leading to Photocurrent Generation*. J. Phys. Chem. B, 2005. **109**(32): p. 15368-15375.
 70. Boens, N., et al., *Rational Design, Synthesis, and Spectroscopic and Photophysical Properties of a Visible-Light-Excitable, Ratiometric, Fluorescent Near-Neutral pH Indicator Based on BODIPY*. Chem.-Eur. J., 2011. **17**(39): p. 10924-10934.
 71. Dodani, S.C., Q. He, and C.J. Chang, *A Turn-On Fluorescent Sensor for Detecting Nickel in Living Cells*. J. Am. Chem. Soc., 2009. **131**(50): p. 18020-18021.
 72. Dexter, D.L., *A Theory of Sensitized Luminescence in Solids*. J. Chem. Phys., 1953. **21**(5):

- p. 836-850.
73. Diring, S., et al., *Star-Shaped Multichromophoric Arrays from Bodipy Dyes Grafted on Truxene Core*. Journal of the American Chemical Society, 2009. **131**(17): p. 6108-6110.
 74. Findlay, N.J., et al., *Linear oligofluorene-BODIPY structures for fluorescence applications*. J. Mater. Chem. C, 2013. **1**: p. 2249-2256.
 75. Hofmann, D.M., et al., *Properties of the yellow luminescence in undoped GaN epitaxial layers*. Phys. Rev. B, 1995. **52**(23): p. 16702-16706.
 76. Bruckbauer, J., *Luminescence study of III-nitride semiconductor nanostructures and LEDs*. 2013, University of Strathclyde.
 77. Bruckbauer, J., et al., *Probing light emission from quantum wells within a single nanorod*. Nanotechnology, 2013. **24**(36): p. 365704-365704.
 78. Kuehne, A.J.C., et al., *Direct Laser Writing of Nanosized Oligofluorene Truxenes in UV-Transparent Photoresist Microstructures*. Advanced Materials, 2009. **21**(7): p. 781-785.
 79. Hong, Y., J.W.Y. Lam, and B.Z. Tang, *Aggregation-induced emission: phenomenon, mechanism and applications*. Chemical Communications, 2009(29): p. 4332-4353.
 80. Zhang, Z., et al., *Color-Tunable Solid-State Emission of 2,2'-Biindenyl-Based Fluorophores*. Angewandte Chemie International Edition, 2011. **50**(49): p. 11654-11657.
 81. Gorrotxategi, P., M. Consonni, and A. Gasse, *Optical efficiency characterization of LED phosphors using a double integrating sphere system*. Journal of Solid State Lighting, 2015. **2**:1.
 82. Zhang, Y. and S.R. Forrest, *Existence of continuous-wave threshold for organic semiconductor lasers*. Physical Review B, 2011. **84**(24): p. 241301.
 83. Ziessel, R. and A. Harriman, *Artificial light-harvesting antennae: electronic energy transfer by way of molecular funnels*. Chemical Communications, 2011. **47**(2): p. 611-631.
 84. Taylor-Shaw, E., et al., *Cool to warm white light emission from hybrid inorganic/organic light-emitting diodes*. J. Mater. Chem. C, 2016. **4**: p. 11499.
 85. Nguyen, T.N., F.M. Ebrahim, and K.C. Stylianou, *Photoluminescent, upconversion luminescent and nonlinear optical metal-organic frameworks: From fundamental photophysics to potential applications*. Coordination Chemistry Reviews, 2018. **377**: p. 259-306.
 86. Lustig, W.P. and J. Li, *Luminescent metal-organic frameworks and coordination polymers as alternative phosphors for energy efficient lighting devices*. Coordination Chemistry Reviews, 2018. **373**: p. 116-147.
 87. Angioni, E., et al., *Implementing fluorescent MOFs as down-converting layers in hybrid light-emitting diodes*. J. Mater. Chem. C, 2019. **7**: p. 2394-2394.
 88. Bai, Y., et al., *Zr-based metal-organic frameworks: design, synthesis, structure, and applications*. Chemical Society Reviews, 2016. **45**(8): p. 2327-2367.
 89. Cavka, J.H., et al., *A New Zirconium Inorganic Building Brick Forming Metal Organic Frameworks with Exceptional Stability*. Journal of the American Chemical Society, 2008. **130**(42): p. 13850-13851.